

ISSN: (Print) (Online) Journal homepage: <https://www.tandfonline.com/loi/tbsd20>

## Statistical analysis/theoretical investigations of novel vascular endothelial growth factor of Davanoide from *Scolymus grandifloras* Desf as potent anti-angiogenic drug properties

Mohammed Semaoui, Fouzia Mesli, Mohammed El Amine Dib, Boufeldja Tabti, Radja Achiri, Jean Costa & Alain Muselli

To cite this article: Mohammed Semaoui, Fouzia Mesli, Mohammed El Amine Dib, Boufeldja Tabti, Radja Achiri, Jean Costa & Alain Muselli (2022) Statistical analysis/theoretical investigations of novel vascular endothelial growth factor of Davanoide from *Scolymus grandifloras* Desf as potent anti-angiogenic drug properties, Journal of Biomolecular Structure and Dynamics, 40:9, 3850-3870, DOI: [10.1080/07391102.2020.1851301](https://doi.org/10.1080/07391102.2020.1851301)

To link to this article: <https://doi.org/10.1080/07391102.2020.1851301>



View supplementary material [↗](#)



Published online: 02 Dec 2020.



Submit your article to this journal [↗](#)



Article views: 76



View related articles [↗](#)




View Crossmark data [↗](#)



Citing articles: 2 View citing articles [↗](#)



# Statistical analysis/theoretical investigations of novel vascular endothelial growth factor of Davanoide from *Scolymus grandifloras* Desf as potent anti-angiogenic drug properties

Mohammed Semaoui<sup>a,b</sup> , Fouzia Mesli<sup>a</sup>, Mohammed El Amine Dib<sup>a</sup>, Boufeldja Tabti<sup>a</sup>, Radja Achiri<sup>a</sup>, Jean Costa<sup>b</sup> and Alain Muselli<sup>b</sup>

<sup>a</sup>Laboratoire des Substances Naturelles & Bioactives (LASNABIO), Département de Chimie, Faculté des Sciences, Université Abou BekrBelkaid, Tlemcen, Algeria; <sup>b</sup>Laboratoire de Chimie des Produits Naturels, UMR CNRS 6134, Université de Corse, Campus Grimaldi, Corte, France

Communicated by Ramaswamy H. Sarma

## ABSTRACT

Many pro-angiogenic factors acting directly or indirectly on the proliferation and differentiation of endothelial cells have been highlighted, in particular: VEGF ('Vascular Endothelial Growth Factor'), FGF ('Fibroblast Growth Factor'), PDGF ('Platelet-Derived Growth Factor'), VEGF exerts its pro-angiogenic activity by binding to the surface of receptors with tyrosine kinase activity (VEGFR). The first objective of this study was to elucidate the composition of the essential oil of the roots of *Scolymus grandifloras* Desf. The second aim was to describe the intra-species variation in essential oil composition in natural populations of 21 oil samples from different Algerian locations using statistical analysis and bioinformatical study of VEGFR inhibition. The essential oil isolated from the root parts, was a really source of Davanoide compounds. The results of the docking simulation revealed that davanone (Ligand 13) has an affinity to interact with cDNA, VEGF and its receptors. The ADMET properties and BOILED-Egg plot validate the compound 13 pass the brain barrier and have high absorption in the intestines with good bioavailability. The findings of this study contribute to the pharmacological knowledge and the therapeutic efficacy of davanone and can initiate the development of new anti-angiogenic drugs. Results showed that essential oil of *Scolymus grandiflorus* presented a large level of percentage of davanone, davanol D1 and 2-hydroxy davanone. These components may be a new source of nontoxic anticancer agents. However, an additional *in vitro* and/or *in vivo* experimental study should make it possible to verify the theoretical results obtained *in silico*.

## ARTICLE HISTORY

Received 3 September 2020  
Accepted 10 November 2020




## KEYWORDS


*Scolymus grandifloras* Desf;  
Davanoide; cancer cells;  
molecular docking;  
molecular dynamic;  
molecular operating  
environment

## 1. Introduction

Cancer has been a disease described since Antiquity. Biologically, cancer results from the occurrence of a dysfunction in certain cells of the body. These start to multiply in an anarchic way and to proliferate, first locally, then in the surrounding tissue, then, at a distance where they form metastases. For decades, scientists could not detect a safe way (or drug) to treat cancer and its connected complications (Chakraborty & Rahman, 2012; Mehrabi et al., 2017). Consequently, try to find or search for new effective anti-cancer agents is a critical strategy in any cancer therapy program. Cancer is never the result of a single cause, but there are a number of factors, external and internal, have been identified. External factors are linked to the environment (radiation, viruses, industrial products, etc.) or lifestyle (tobacco, alcohol, food, etc.). Internal factors are linked to age and inheritance. Without forgetting the genetic predisposition to cancer (special case of inherited mutations) the best-known concern the BRCA1 and BRCA2 genes; they

generate a significant risk of breast and ovarian cancer. Medicinal plants possess a characteristic that helps in food security and treating diseases by improving people's health conditions. These plants produce substances that are capable to altering the synthetic compounds already existed, so they become an excellent source to research a new compound for therapeutic use. With an area of over 2.3 million km<sup>2</sup>, Algeria is the largest country in the Mediterranean basin. It presents a great plant biodiversity which amounts to more than 1600 species. The genus *Scolymus* belonging to Asteraceae family including three species: *Scolymus hispanicus* L., *Scolymus maculatus* L. and *Scolymus grandifloras* Desf (Quezel et al., 1962). In Sicily, these wild species are commonly consumed in salads (Guarrera & Savo, 2016), they are distributed in the Mediterranean, Macaronesia and Near-Eastern zones (Vázquez, 2000). To our knowledge, there are no chemical studies on the species *S. grandiflorus*. The most studied species belonging to this genus is *S. hispanicus* commonly called 'Golden thistle', locally called 'Ghernina'. This

**CONTACT** Mohammed El Amine Dib  [a\\_dibdz@yahoo.fr](mailto:a_dibdz@yahoo.fr)  Laboratoire des Substances Naturelles & Bioactives (LASNABIO), Département de Chimie, Faculté des Sciences, Université Abou BekrBelkaid, Tlemcen, Algeria; Fouzia Mesli [meslifouzia2018@gmail.com](mailto:meslifouzia2018@gmail.com)  Laboratoire des Substances Naturelles & Bioactives (LASNABIO), Département de Chimie, Faculté des Sciences, Université Abou BekrBelkaid, BP 119, Tlemcen 13000, Algeria.

 Supplemental data for this article can be accessed online at <https://doi.org/10.1080/07391102.2020.1851301>

Codes	Stations	Latitude	Longitude	Altitudes
Y1	El Ourit	34°52'41"N	1°15'05"W	818 m
Y2	Sebdou	34°42'05"N	1°18'46"W	1100 m
Y3	Ain fezza centre	34°51'53"N	1°13'22"W	900 m
Y4	Temi ben hadiel	34°48'24"N	1°23'21"W	1163 m
Y5	Maaziz	34°56'24"N	1°48'14"W	880 m
Y6	Oum el' Alou	34°55'05"N	1°11'24"W	858 m
Y7	Tizi	34°54'24"N	1°10'00"W	800 m
Y8	Sabra	34°48'57"N	1°31'44"W	610 m
Y9	Ouled Mimoun	34°55'16"N	1°03'30"W	620 m
Y10	Beni snous	34°40'56"N	1°30'34"W	680 m
Y11	Bouhlou	34°47'36"N	1°35'02"W	531 m
Y12	Azayza	34°59'08"N	1°10'41"W	600 m
Y13	Maghnia 2	34°54'04"N	1°44'39"W	440 m
Y14	Sidi Abdeli	35°03'11"N	1°08'59"W	510 m
Y15	Ain El Hout	34°57'13"N	1°19'15"W	360 m
Y16	Sidi Medjahed	34°46'48"N	1°40'04"W	434 m
Y17	Bensekrane	35°03'58"N	1°13'45"W	300 m
Y18	Fellaoucen	35°03'47"N	1°32'51"W	170 m
Y19	Zenata	35°01'14"N	1°27'32"W	275 m
Y20	Maghnia	34°49'33"N	1°41'22"W	380 m
Y21	Nedroma	35°03'10"N	1°45'29"W	185 m

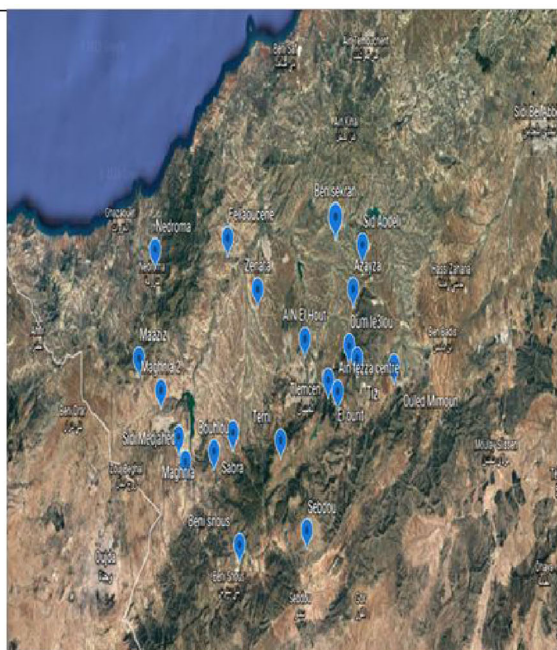


Figure 1. Geographical distribution of *S. grandiflorus* from western Algeria.

species is one of the most appreciated-consumed wild vegetables in Mediterranean countries, recognized for their medicinal properties such as diuretic, depurative, digestive, choleric and lithiuretic (Polo et al., 2009).

Our study was about *S. grandiflorus* originally of north-Africa (Martin & Ruperté, 1979) described for the first time by Desfontaines (1800). Several new molecules, targeting cell proliferation and/or angiogenesis have been recently tested, whose modest effectiveness nevertheless allows us to foresee a new global approach to this pathology. Indeed, these new treatments go beyond the classical chemo- or radio-therapeutic perspective of blocking cell replication at the level of DNA and its machinery, by targeting intracellular signaling mechanisms, intercellular paracrine connections or even the tumor micro-environment. The main interest was to develop unique potential inhibitors of the VEGF (Vascular Endothelial Growth Factor)/VEGFR interaction, the earlier a cancer is treated, the less the treatments are heavy and the better the chances of cure. The previous works of Ravi and Krishnan (2016) proved that *N*-hexadecanoic acid extracted from *Kigelia pinnata* leaves has high affinity interaction with DNA topoisomerase-I and the research of Hosseinzadeh et al. (2019) proved that hydroperoxide of davanone a potential antitumor agent.

Furthermore, modeling and simulation have become standard practices in many scientific and technical fields and in particular in Chemistry. They are often necessary when the real experience is too difficult, too dangerous and too expensive. Digital chemistry subsidizes a better understanding of the action of medicinal plants against diseases and offers high-level training, focused on the study of living things at the molecular level. In addition, represents a bridge between theory and experience. It makes it possible to represent, interpret and predict biomolecular structures and functions (Mesli et al., 2019). However, there are no reports on

chemical composition and biological activities of *S. grandiflorus*. Therefore, this work was aimed to study for the first time, the chemical composition from root parts and the intraspecies variations of essential oils from 21 locations using statistical analysis and the second study was to try to tested the molecules of this oil for their anticancer activity by interested at the interaction between VEGF and its receptors (VEGFR). Knowing that VEGF seems to be one of the main players in tumor angiogenesis. It exerts its pro-angiogenic activity by binding to the surface of receptors with tyrosine kinase activity (Walker, 1996). The essential oils of *S. grandiflorus* roots inhibitors were the subject of our investigation. In order to block tumor growth and we target receptors (VEGFR). These receptors have different affinities for VEGF and induce different cellular and biological effects. The inhibition of VEGF receptors was theoretically investigated by two methods of computational chemistry: molecular docking analyzes and molecular dynamics (MD) simulations. In this contribution, a combined of three theoretical approaches by using drug likeness, pharmacokinetics, medicinal Chemistry and ADME Properties to explore potential inhibitors among compounds of essential oils of *S. grandiflorus* roots against three enzymes: VEGF, VEGFR1 and VEGFR2.

## 2. Material and methods

### 2.1. Plant material and isolation of the essential oil

Roots of *S. grandiflorus* were collected at the flowering stage in May 2018 from 21 locations (Y1–Y21) widespread in two areas of western Algeria (Tlemcen), (Y1–Y7) from Tell mountain and (Y8–Y21) from littoral (Figure 1).

The plant material was botanically identified by Prof. Noury Benabadji (Laboratory of Ecology and Ecosystem Management of University of Tlemcen Algeria) (Mejdoub et al., 2020). Voucher specimens were installed with the Herbarium of the University of

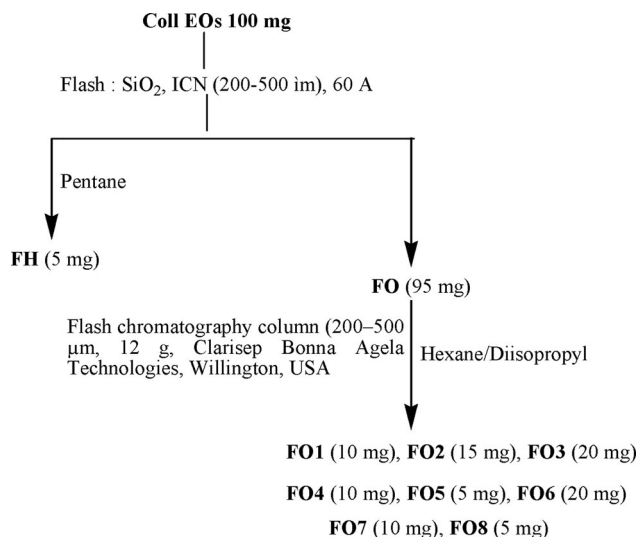


**Figure 2.** Fractionation of Coll EOs from roots *S. grandiflorus*.

Tlemcen. The root parts were air-dried at room temperature. The plant material from each population was submitted to hydro-distillation for 5 h using a Clevenger apparatus according to the procedure described in the European Pharmacopeia (Conseil de l'Europe, 1996). The isolated essential oils were dried over anhydrous sodium sulfate  $\text{Na}_2\text{SO}_4$ , filtered and then the essential oil mass was determined.

## 2.2. Fractionation of collective essential oil

One (1) g of Coll EOs was subjected to fractionation flash chromatography ( $\text{SiO}_2$ , ICN 200–500 mm, 60 A). By elution with pentane, an FH fraction containing the hydrocarbon compounds (5 mg) was obtained; elution with diethyl ether then leads to an FO fraction containing the oxygenated compounds (95 mg). The oxygenated fraction (95 mg) were submitted to fractionation on silica flash chromatography column (200–500  $\mu\text{m}$ , 12 g, ClarisepBonna-Agela Technologies, Wellington, USA) using an Automated Combi Flash apparatus (Teledyne ISCO, Lincoln, USA), equipped with automatic fraction collector monitored by an UV detector, eluted with a gradient of hexane (A) and di-isopropyl ether (B) from: (A: 100%; B: 0%) to (A: 0%; B: 100%). eight fractions were obtained and submitted to GC–FID, GC–MS and nuclear magnetic resonance (NMR) analyses. The fractionation is shown schematically in (Figure 2).

### FO1 (5,5-Dimethyl-2(5H)-furanone):

$^1\text{H}$  NMR (400 MHz,  $\text{CDCl}_3$ )  $\delta$  1.49 (6H, s), 5.98–5.99 (1H, d,  $J = 5.6$  Hz), 7.39–7.40 (1H, d,  $J = 5.6$  Hz).

$^{13}\text{C}$  NMR (101 MHz,  $\text{CDCl}_3$ )  $\delta$  25.4, 86.6, 119.9, 161.2, 172.5.

HRMS calcd for  $\text{C}_6\text{H}_8\text{O}_2$  :112.13, found: 112; LRMS (EI +)  $m/z$  ; 97 (100), 69 (80),43 (80), 26 (30).

### FO3 (Davana furan):

$^1\text{H}$  NMR (400 MHz,  $\text{CDCl}_3$ )  $\delta$  1.20 – 1.21 (d, 3H), 1.29 (s, 3H), 1.75 (m, 2H), 1.87 (m, 2H), 2.25(s, 3H), 3.02 (m,  $J = 7.3$ , 6.9 Hz, 1H), 4.29–4.20 (q, 1H), 4.97 (dd,  $J = 10.7$ , 6.8, 1.6 Hz, 1H), 5.22–5.17 (dd, 1H), 5.88 (s, 1H), 5.90 (s, 1H), 5.99–5.92 (m, 3H).

$^{13}\text{C}$  NMR (101 MHz,  $\text{CDCl}_3$ )  $\delta$  13.6, 14.2, 26.0, 28.1, 37.8, 37.9, 81.2, 82.7, 105.6, 105.8, 111.4, 144.5, 150.2, 156.1.

HRMS calcd for  $\text{C}_{14}\text{H}_{20}\text{O}_2 \sim 220.1478$ , found: 220; LRMS (EI +)  $m/z$ ; 220(20), 135(20), 111(30), 109(100), 93(30), 55(30), 43(40).

### FO5 (Davanone):

$^1\text{H}$  NMR ( $\text{CDCl}_3$ , 400 MHz)  $\delta$  0.96–1.04 (3H, d,  $J = 6.9$  Hz), 1.23–1.28 (3H, s), 1.52–1.65 (1H, m), 1.62 (3H, s), 1.63 (3H, s,  $J = 3.8$  Hz), 1.68–1.80 (1H, m), 1.84–1.95 (1H, m), 1.95–2.07 (1H, dddd,  $J = 3.6$ , 5.8, 7.2, 11.9 Hz), 2.65–2.76 (1H, dq,  $J = 6.9$ , 8.8 Hz), 3.15–3.37 (2H, m), 4.04–4.14 (1H, td,  $J = 5.8$ , 8.7 Hz), 4.94–5.03 (1H, dd,  $J = 1.7$ , 10.7 Hz), 5.15–5.26 (1H, dd,  $J = 1.7$ , 17.2 Hz), 5.29–5.39 (1H, tdq,  $J = 1.5$ , 2.9, 7.2 Hz), 5.84–5.96 (1H, dd,  $J = 10.7$ , 17.3 Hz)

$^{13}\text{C}$  NMR (101 MHz,  $\text{CDCl}_3$ )  $\delta$  13.2, 18.1, 25.7, 26.6, 29.9, 37.6, 42.7, 51.3, 81.0, 83.0, 111.4, 116.1, 135.4, 144.7, 212.1.

HRMS calcd for  $\text{C}_{15}\text{H}_{24}\text{O}_2 \sim 236.18$ , found: 236; LRMS (EI +)  $m/z$  180 (20), 125 (20), 111 (100), 93 (90), 69 (80), 55 (70), 41 (60).

### FO7 (2-Hydroxy davanone):

$^1\text{H}$  NMR ( $\text{CDCl}_3$ , 400 MHz)  $\delta$  1.01–1.08 (3H, d,  $J = 7.0$  Hz), 1.22–1.31 (3H, d,  $J = 2.6$  Hz), 1.35–1.41 (6H, d,  $J = 1.7$  Hz), 1.60–1.70 (1H, ddt,  $J = 8.0$ , 9.2, 11.9 Hz), 1.72–1.80 (1H, ddd,  $J = 7.1$ , 9.2, 12.0 Hz), 1.85–1.96 (1H, ddd,  $J = 3.9$ , 7.8, 11.7 Hz), 1.96–2.07 (1H, m), 2.15–2.20 (2H, s), 2.90–2.98 (1H, dd,  $J = 7.0$ , 8.3 Hz), 4.18–4.28 (1H, td,  $J = 6.0$ , 8.3 Hz), 4.93–5.01 (1H, dd,  $J = 1.7$ , 10.7 Hz), 5.13–5.22 (1H, dd,  $J = 1.6$ , 17.2 Hz), 5.82–5.96 (1H, m), 6.38–6.46 (1H, d,  $J = 15.7$  Hz), 6.88–6.96 (1H, d,  $J = 15.7$  Hz).

$^{13}\text{C}$  NMR (101 MHz,  $\text{CDCl}_3$ )  $\delta$  13.1, 25.4, 26.5, 29.3, 29.4, 29.4, 37.6, 49.9, 71.9, 80.5, 83.0, 111.5, 125.2, 144.6, 152.5, 202.9.

HRMS calcd for  $\text{C}_{15}\text{H}_{24}\text{O}_3$  : 252.17, found ([M+] $^-$  -  $\text{H}_2\text{O}$ ) : 237 ; LRMS (EI +)  $m/z$  166 (20), 138 (20), 125 (30), 113 (80), 111 (80), 93 (90), 85 (60), 67 (40), 55 (70), 43 (100).

## 2.3. Identification of the oil components

### 2.3.1. Gas chromatography

The gas chromatography (GC) analysis was carried out using Clarus 500 Perkin-Elmer Auto system apparatus equipped by two flame ionization detectors (FID), with a fused capillary columns (50 m  $\times$  0.22 mm I.D; film thickness 0.25  $\mu\text{m}$ ), BP-1 (polymethyl-siloxane) and BP-20 (polyethylene glycol); carrier gas, helium; linear velocity, 0.8 mL/min (Bekhechi et al., 2010). The oven temperature was fixed from 60  $^\circ\text{C}$  to 220  $^\circ\text{C}$  at 2  $^\circ\text{C}/\text{min}$  and then held isothermal (20 min). Injector temperature was 250  $^\circ\text{C}$  (injection mode: split 1/60); detector temperature 250  $^\circ\text{C}$ . The relative proportions of the essential oil constituents were expressed as percentages obtained by peak area normalization, without using correction factors, as described previously (Medbouhi et al., 2018).

### 2.3.2. Gas chromatography/mass spectrometry

Essential oils were analyzed with a PerkinElmer Turbo-Mass quadrupole analyzer, coupled to a PerkinElmer Autosystem XL, equipped with two fused-silica capillary columns and

operated with the same GC conditions described above, except for a split of 1/80. EI mass spectra were acquired under the following conditions: Ion source temp. 150 °C, energy ionization 70 eV, mass range 35–350 Da (scan time: 1 s) (Tabet Zatlá et al., 2017).

### 2.3.3. Nuclear magnetic resonance

NMR spectroscopy experiments on the fractions were performed on a Bruker AVANCE 400 Fourier Transform spectrometer operating at 100.13 MHz ( $^{13}\text{C}$ ), equipped with a 5 mm probe, in deuterated chloroform ( $\text{CDCl}_3$ ), with all shifts specified to internal tetramethyl silane (TMS). Spectra were recorded with the following parameters: pulse width (PW), 4  $\mu\text{s}$  (flip angle 45°); acquisition time, 2.7 s for 128 K data table with a spectral width (SW) of 24,000 Hz (240 ppm); CPD mode decoupling; digital resolution 0.183 Hz/pt (Esselin et al., 2017). The number of accumulated scans ranged was 3000 for each sample (50–60 mg in 0.5 mL of  $\text{CDCl}_3$ ) (Bouzabata et al., 2010).

## 2.4. Theoretical background and computational details

### 2.4.1. Targets and compounds preparations

In this study, the interactions of essential oils of *S. grandiflorus* roots from compounds were investigated. The structures of inhibitors were downloaded from the PubChem database (<https://pubchem.ncbi.nlm.nih.gov>). The PDB database (<https://www.rcsb.org/>) were used to obtain the complete structure of vascular endothelial growth factor receptors (VEGFR-1) (PDB ID: 3HNG (Tresaugues et al., 2013)), VEGFR-2 (PDB ID: 2XIR (Marrone et al., 2007)), VEGF (PDB ID: 5T89 (Markovic-Mueller et al., 2017)) was obtained by X-ray diffraction method).

### 2.4.2. Molecular docking

In this research, specific molecular operating environment (MOE) was used to study the molecular interaction between essential oils of *S. grandiflorus* roots compounds and the vascular endothelial growth factor receptors (VEGFR-1, VEGFR-2 and VEGF) enzymes. During this molecular docking study, the number of interactions was 10, the cut-off for coulomb interaction and van der Waal interaction was (about 30 angstrom) with the ability to study the hydrogen-electrostatic in the total active site of the enzyme was validated and the results were discussed. The present research aimed at indicating the binding mode of essential oils of *S. grandiflorus* roots compounds into the three targets VEGFR-1, VEGFR-2 and VEGF worming molecular docking. The energy of the enzyme was minimized and geometry was conducted using Hamiltonian implanted in MOE software and then isolation of the active site of the target. The most stable geometry of each compound was minimized by the same semi-empirical method (AM1) (Stewart, 2007). All simulations were run by using all explicit salvation models using TIP3P water. After that, the binding energy between ligands and targets was calculated and based on molecular mechanics (Halgren, 1996, 1999).

### 2.4.3. MD simulation

The favorite conformer of Vascular Endothelial Growth Factor receptors with compounds was subjected to MDs Simulations MD was achieved for both the complex (3HNG, 2XIR, 5T89) adopting the MOE software (Al-Haderet et al., 1993). Dynamics simulation needs the Nose–Poincaré–Andersen (NPA) equations of motion (Bond et al., 1999; Sturgeon, & Laird, 2000). The coordinates were saved every 0.2 ps to get an accurate view of molecular movement. MDs simulations require the Berendsen thermostat to rescale the velocities of particles (Berendsen et al., 1984). In all simulations the van der Waals cut-out distance was set to 8 Å. Energy minimization process was activated by using MMFF94x force field (Parikesit et al., 2015). We have shown the detailed analysis of (MD) simulation results of only compound L25 with target VEGF receptors because these compounds show superior binding affinity for both VEGF receptors. At last and according to (MD) simulation analysis among these two compounds the most effective molecules were L25 and L13 (Graphical MD for ligand 13 [see Supporting Information Figures 15–17]) in VEGF receptors. The MOE software was used for our study because it has proven its performance in several recent studies; we can cite some example of work: Naz et al. (2020), Stitou et al. (2020), Daoud et al. (2018), Ghufuran et al. (2019) and Mesli and Ghalem (2017).

## 3. Results and discussion

### 3.1. Composition of the Coll EO and yields

The essential oil *S. grandiflorus* roots collected in Tlemcen from Western Algeria, afforded pale yellow oil with average yield varied of 0.07% to 0.08% (w/w) based on the dry mass of the plant. Preliminary analysis of the essential oils of *S. grandiflorus* obtained from the roots of 21 sites (Table 1) was identified only 10 compounds by comparing their mass spectra (EI-MS) and retention indices (RIs) with those of mass-spectral library (Arome) and by comparison of their mass spectra and RIs with those listed in commercial mass-spectral libraries (Table 1). The compounds identified in the Coll EO were Lavender lactone (1.5%), cis-Arbusculon (2.1%), trans-Arbusculon (0.9%), cis-Linalool oxide (0.4%), E- $\beta$ -Elemene (0.5%), iso davanone (1.6%), davanol D1 (6.5%), Eudesma-11-en-4 $\alpha$ -ol, (2.1%) Tetradecanoic acid (0.8%) and hexadecanoic acid (0.8%; Table 1). All individual oil samples were pooled to produce a 'collective essential oil' (EO Coll.) that was used to perform detailed analysis using successive column chromatography (CC), GC (RI), GC/MS and NMR analysis (Table 1). Flash Chromatography of oxygenated fraction (FO) afforded eight fractions of the total Coll Eos, in order of their elution (Figure 2). The analysis by GC-MS and NMR of the oxygenated fractions by comparison with the different fragments (GC-MS) and chemical shifts (NMR) with those of the literature (Alwahibi et al., 2016; Naegeli & Weber, 1970; Thomas et al., 1974; Wan et al., 2013) (see material and methods) showed that fraction **FO1** contained the component of 5,5-dimethyl-2(5H)-furanone with percentage of 89.7%, **FO3** contained four stereoisomers of Davana furan (5.9% (1), 11.3%

Table 1. Percentage of compounds identified in the essential oils of *S. grandiflorus* isolated from various localities.

No	Compounds	b <sub>1</sub> R <sub>1</sub> a	s <sub>1</sub> R <sub>1</sub> a	d <sup>1</sup> R <sub>1</sub> p	Id. Methods	Col.EO	Stations																							
							Y1	Y2	Y3	Y4	Y5	Y6	Y7	Y8	Y9	Y10	Y11	Y12	Y13	Y14	Y15	Y16	Y17	Y18	Y19	Y20	Y21	Y21		
1	5,5-dimethyl Furanone	914	919	1594	IR, MS, <sup>13</sup> C RMN	2.9	5.5	5.5	6.3	6.6	5.9	7.5	9.0	3.4	2.5	2.8	2.1	2.2	1.2	1.5	1.1	0.6	0.6	0.9	1.1	1.6	1.0			
2	Lavender lactone	1002	996	1647	IR, MS, ref	1.5	2.2	3.9	3.1	2.9	1.9	2.2	3.2	1.0	0.5	1.1	0.4	0.7	0.3	0.6	0.4	0.3	0.2	0.3	0.8	0.6	0.3			
3	cis-Arbusculon	1052	1032	1442	IR, MS, ref	2.1	1.9	0.5	1.6	0.7	2.7	4.9	5.6	2.1	1.7	1.7	1.2	1.9	0.6	1.1	0.8	0.8	0.3	0.6	1.1	1.1	0.8			
4	trans-Arbusculon	1071	1048	1481	IR, MS, ref	0.9	1.5	0.7	1.3	0.6	1.9	3.7	3.4	1.4	0.9	1.1	0.8	1.2	0.7	0.8	0.6	0.4	0.3	0.4	0.7	1.1	0.4			
5	cis-Linalool oxide	1065	1055	1493	IR, MS, ref	0.4	0.2	0.5	0.3	0.4	0.3	0.3	0.2	0.1	0.1	0.3	0.4	0.1	0.3	0.4	0.3	0.6	0.2	0.2	0.5	0.4	0.3			
6	Davanafuran (1)	/	1371	1702	IR, MS	0.2	0.3	0.2	0.4	0.3	0.4	0.2	0.4	0.3	0.2	0.1	0.2	0.5	0.5	0.4	0.3	0.2	0.2	0.2	0.4	0.4	0.3			
7	Davanafuran (2)	/	1379	1722	IR, MS	0.7	1.1	0.2	0.7	0.5	1.1	0.7	0.5	0.3	0.4	0.5	0.4	0.3	0.2	0.9	0.1	0.3	0.6	0.4	0.5	0.7	0.2			
8	Davanafuran (3)	/	1383	1729	IR, MS	0.4	0.4	0.3	0.3	0.3	0.3	0.5	0.4	0.2	0.7	0.2	0.2	0.3	0.6	0.6	0.4	0.4	0.2	tr	0.1	0.2	0.6			
9	E-β-Elementene	1387	1389	1593	IR, MS, ref	0.5	0.9	0.4	0.1	0.6	1.3	0.2	0.4	0.3	0.4	0.4	0.4	0.4	0.3	0.1	0.7	0.7	0.7	0.6	0.3	0.3	0.6			
10	Davanafuran (4)	1393	1394	1766	IR, MS, <sup>13</sup> C RMN	2.6	2.0	2.5	1.3	3.5	2.3	3.0	2.3	2.0	2.7	2.3	3.9	2.2	2.2	3.2	2.6	3.2	0.9	1.7	1.4	3.6	3.4			
11	Davana ether (1)	/	1466	1890	IR, MS, ref	0.8	0.2	0.7	tr	0.6	0.1	0.2	0.3	0.2	0.8	0.3	0.4	0.7	0.5	1.2	1.2	1.3	0.2	0.1	0.3	1.7	1.2			
12	Davana ether (2)	/	1474	1908	IR, MS, ref	2.1	0.5	0.5	0.5	0.7	0.7	0.6	0.5	0.7	0.3	1.0	0.7	2.2	3.7	4.5	3.1	4.1	2.3	2.2	1.1	5.3	3.2			
13	Davanone (1)	/	1534	1955	IR, MS	1.1	1.0	0.2	0.3	0.3	1.4	0.7	0.3	0.4	0.9	0.6	0.4	1.1	1.4	2.4	1.6	1.9	1.3	1.2	0.3	2.8	1.4			
14	Davanone (2)	/	1540	1973	IR, MS	1.1	0.7	0.3	0.5	0.2	0.9	0.7	0.7	0.9	1.9	1.1	1.0	1.7	0.4	1.4	1.6	1.5	1.8	1.5	0.8	1.3	2.2			
15	Iso davanone	1562	1537	/	IR, MS, ref	1.6	0.7	0.9	0.5	1.2	0.5	0.9	1.1	1.1	2.5	1.3	1.3	2.0	1.7	1.9	2.1	1.5	2.2	2.4	1.1	1.9	1.7			
16	Davanone (3)	/	1546	1994	IR, MS	1.8	1.4	0.4	1.1	0.7	1.1	1.5	1.3	1.4	2.7	1.6	1.7	2.2	2.9	2.7	2.0	1.1	1.8	2.2	1.9	1.7	2.0			
17	Davanone (4)	1569	1570	2035	IR, MS, <sup>13</sup> C RMN	45.3	24.4	19.9	26.4	23.0	27.8	30.6	35.0	51.9	45.0	51.0	45.8	49.6	53.7	41.3	52.7	50.4	73.2	68.4	61.5	48.4	54.5			
18	Davanol D1	1591	1602	2090	IR, MS	6.5	2.4	4.9	4.0	6.2	3.6	3.5	2.0	2.9	5.8	3.5	3.2	6.7	2.1	3.1	4.9	2.7	2.8	3.3	2.5	2.3	5.3			
19	Eudesma-11-en-4α-ol	1642	1638	2233	IR, MS	2.1	1.8	4.0	3.7	2.9	1.9	1.1	0.8	2.3	1.4	1.9	2.7	1.8	1.8	2.2	1.7	1.1	1.7	2.1	1.8	1.0	1.4			
20	2-Hydroxy davanone (1)	/	1644	2496	IR, MS	0.1	0.5	0.1	0.2	0.2	0.3	0.4	0.4	0.3	0.1	0.1	0.1	0.1	0.1	0.2	0.3	0.4	0.9	0.8	0.1	0.2	0.2			
21	2-Hydroxy davanone (2)	/	1657	2513	IR, MS	0.4	1.4	0.9	0.9	1.3	1.7	1.3	0.8	0.4	0.5	0.3	0.2	0.6	0.4	0.5	0.2	0.2	0.3	0.3	0.1	0.3	0.1			
22	2-Hydroxy davanone (3)	/	1665	2531	IR, MS	5.3	4.3	3.2	5.2	4.2	3.9	2.1	1.7	1.3	1.3	1.2	0.9	1.2	0.8	0.9	0.6	0.6	0.7	1.0	0.2	0.5	0.7			
23	2-Hydroxy davanone (4)	1668	1682	2566	IR, MS, <sup>13</sup> C RMN	11.2	26.1	33.2	23.1	29.8	23.9	19.7	14.0	10.8	8.7	5.7	5.1	6.1	1.8	2.4	2.5	2.2	1.8	2.7	3.1	2.3	2.8			
24	Tetradecanoic acid	1748	1745	2682	IR, MS	0.8	0.3	0.2	0.2	0.4	0.2	0.3	0.2	0.4	0.3	0.2	0.3	0.4	0.7	0.6	0.6	0.3	1.3	1.0	0.7	tr	0.5			
25	Hexadecanoic acid	1942	1942	2628	IR, MS	0.8	0.5	0.3	0.2	0.6	0.3	0.7	0.4	9.5	8.5	10.2	12.5	9.8	13.1	11.5	8.6	15.2	3.2	3.8	8.9	16.8	10.3			
<b>% Total identification</b>							<b>93.2</b>	<b>82.2</b>	<b>84.4</b>	<b>82.2</b>	<b>88.7</b>	<b>86.4</b>	<b>87.5</b>	<b>84.9</b>	<b>95.6</b>	<b>92.8</b>	<b>86.3</b>	<b>96.0</b>	<b>92.0</b>	<b>86.7</b>	<b>91.0</b>	<b>92.1</b>	<b>99.7</b>	<b>98.3</b>	<b>91.3</b>	<b>96.1</b>	<b>95.4</b>			
Hydrocarbon sesquiterpenes							0.5	0.9	0.4	0.1	0.6	1.3	0.2	0.4	0.3	0.4	0.4	0.4	0.3	0.1	0.7	0.7	0.7	0.7	0.6	0.3	0.3	0.6		
Oxygenated monoterpenes							0.4	0.2	0.5	0.3	0.4	0.3	0.3	0.2	0.1	0.1	0.3	0.4	0.1	0.3	0.4	0.3	0.4	0.3	0.6	0.2	0.2	0.5	0.4	
Oxygenated sesquiterpenes							79.4	65.4	69.2	64.0	71.3	67.8	63.3	58.9	74.6	73.9	69.6	63.5	76.0	71.3	65.0	74.5	69.0	91.0	88.2	74.8	69.7	76.7	67.7	76.7
Non-terpenic oxygenated compounds							12.9	15.7	14.3	15.4	16.4	17.0	23.7	25.4	20.6	18.4	20.2	22.0	19.5	20.1	21.2	15.5	21.8	7.8	9.3	15.7	25.7	17.8	17.8	

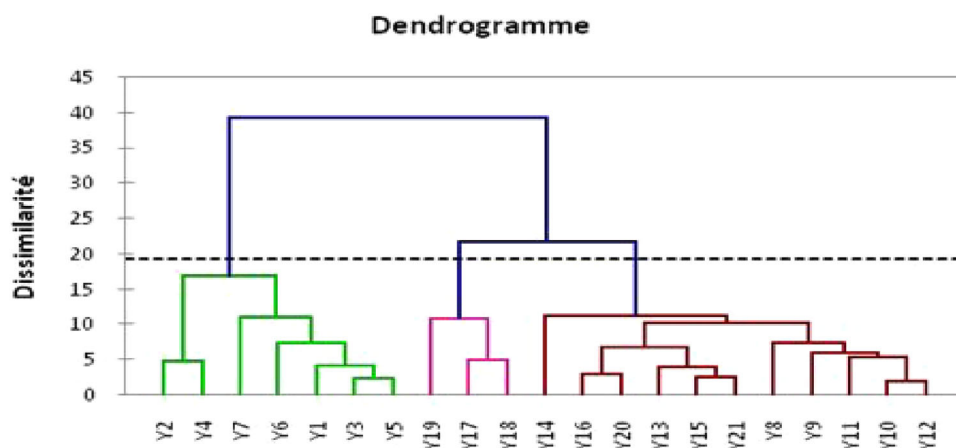


Figure 3. Cluster analysis (CA) of chemical compositions of *S. grandiflorus* from Algeria.

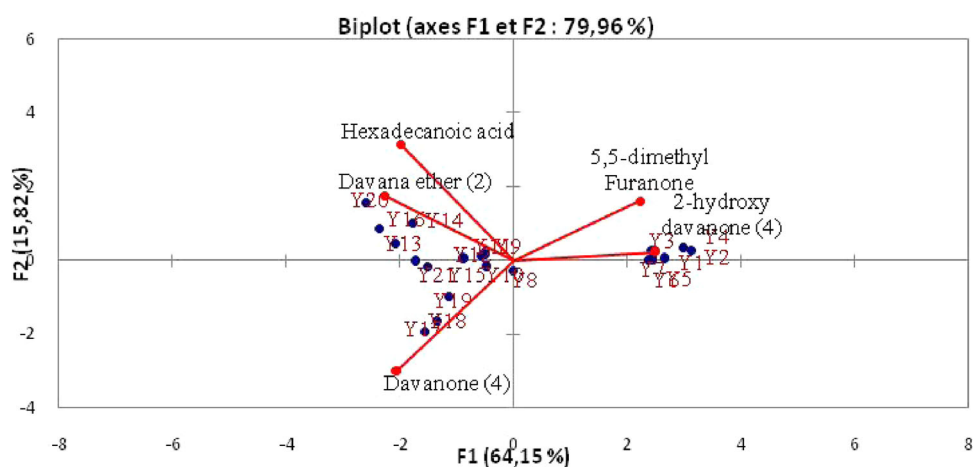


Figure 4. Principal component analysis (PCA) of chemical compositions of *S. grandiflorus*.

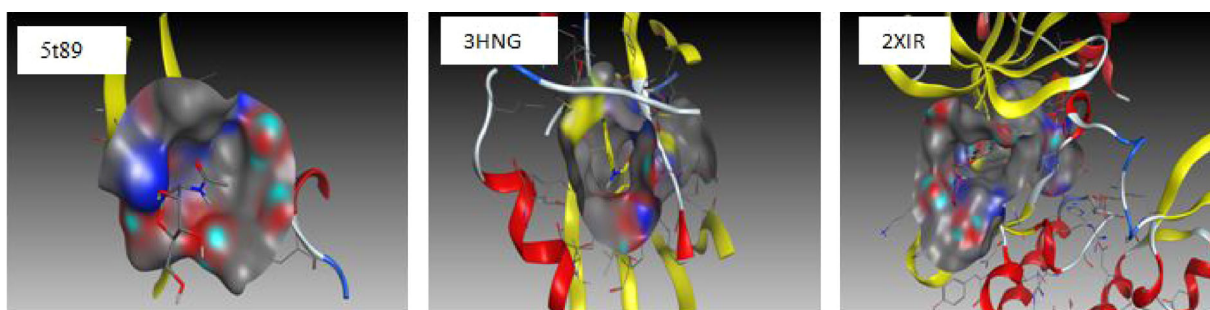


Figure 5. Enzymatic cavity with the residues of the active site for the targets: 5T89, 3HNG and 2XIR.

(2), 2.6% (3) and 66.5% (4)), **FO4** contained davanol (D) (88.2%) and Fraction **FO5** contained four stereoisomers of davanone (6.2% (01), 7.5% (2), 7.2% (3) and 75.7% (4)) and Fraction **FO7** contained four stereoisomers of 2-hydroxy davanone (0.8% (1), 6.2% (2), 10.4% (3) and 63.3% (4)) (Table 1). The most abundant davanoid was cis-davanone, Natural (+)-davanone, a sesquiterpenoid ketone that was first isolated from *Artemisia pallens* (Sipma & Van der Wal, 2010). Davanone was the main constituent of several species of *Artemisia* species of the Asteraceae family. The major component of essential oils of aerial parts of *Artemisia ciniformis* (Rustaiyan et al., 2007). *Artemisia kermanensis*, *Artemisia kopetdaghensis* and *Artemisia khorassanica* of Iran (Ramezani

et al., 2005; Rustaiyan et al., 2009) and also identified in the leaves and flowers of *Lantana camara* L (El Baroty et al., 2014; Saikia & Sahoo, 2011).

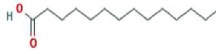
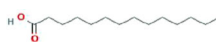
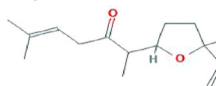
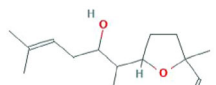



### 3.2. Chemical variability of *S. grandiflorus* essential oils

Twenty-one wild populations (Y1 to Y21) of *S. grandiflorus* were collected during flowering with different altitudes. Seven samples (S1–S7) at high altitude (600–1100 m) with an important precipitation, located in Tlemcen mountains and fourteen stations (S8–S21) at low altitude (170 m to 500 m) in littoral of Tlemcen with low precipitation (Table 1, Figure 1).

**Table 2.** Some properties of all compounds for anti-angiogenic drug.

Ligand Compound	Toxic	LogP	Energies (Kcal/mol)	LogS	Hdon + Hacc	Flexibility
L01 5.5-dimethyl Furanone	No	1.70	1.82361 e+ 001	-1.18	don:0; acc:2	3 out 3
L02 Lavender lactone	No	1.27	8.81161 e+ 000	-1.05	don:0; acc:1	1 out 1
L03 Cis-Arbusculon	No	1.70	2.65666 e+ 001	-1.45	don:0; acc:2	2 out 2
L04 Trans-Arbusculon	No	1.70	2.73648 e+ 001	-1.45	don:0; acc:2	2 out 2
L05 cis-Linalool oxide	No	1.88	3.73575 e+ 001	-1.56	don:1; acc:2	2 out 2
L06 Davanafuran	No	3.51	2.49849 e+ 001	-2.89	don:0; acc:0	2 out 2
L09 (E)- $\beta$ -Elemene	No	4.75	4.43553 e+ 001	-6.04	don:0; acc:0	3 out 3
L11 Davana ether	No	3.75	2.97817 e+ 001	-3.03	don:0; acc:2	2 out 2
L13 Davanone	No	3.67	3.22538 e+ 001	-2.88	don:0; acc:2	5 out 5
L15 Iso davanone	No	3.67	3.10733 e+ 001	-2.88	don:0; acc:2	5 out 5
L18 Davanol D1	No	3.46	3.72150 e+ 001	-2.66	don:1; acc:2	5 out 5
L19 Eudesma-11-en-4 $\alpha$ -ol	No	3.92	4.83154 e+ 001	-4.36	don:1; acc:1	1 out 1
L20 2-Hydroxy davanone	No	2.64	3.23785 e+ 001	-2.48	don:1; acc:3	5 out 5
L24 Tetradecanoic acid	No	4.77	-1.4216 e+ 001	-5.46	don:1 acc:2	12 out 12
L25 Hexadecanoic acid	No	5.55	-1.4606 e+ 001	-6.49	don:1; acc:2	14 out 14

**Table 3.** Results of bonds between atoms of best compounds and active site residues of three targets.

No	Chemical structure	S-score (Kcal/mol)	Bonds between atoms of compounds and residues of the active site				Distances (Å)	Energies (Kcal/mol)
			Atom of compound	Involved receptor atoms	Involved receptor residues	Type of interaction bond		
L24		-3.809	O1 1	N	LEU 97	H-acceptor	2.82	-3.4
			O1 1	NH2	ARG 56	ionic	3.99	-0.5
L25		-4.003	O1 1	N	LEU 97	H-acceptor	2.90	-2.8
L13		-6.529	O1 1	N	ASP 1040	H-acceptor	2.93	-3.4
L18		-7.345	C6 6	6-ring	PHE 1041	H-pi	4.27	-0.8
L24		-7.470	O1 1 O1 1	NE	ARG 1021 ARG	H-acceptor H-	2.87	-5.8
			O2 2	NH2	1021 ARG 1021	acepr	2.99	-4.0
			O2 2 O1 1 O1 1	NH2	HOH 3024 ARG	H-accor	3.26	-3.7
			1 O2 2	O	1021 ARG 1021	-acceptor ionic	3.24	-1.3
				NE	ARG 1021	ionic	2.87	-5.4
L25		-8.504	O1 1 O1 1	NE	ARG 1021 ARG	H-acceptor H-	3.03 2.83 3.03	-5.3
			O2 2 O2 2 O1 1	NH2	1021 ARG 1021	acceptor ionic	3.45 3.93 2.83	-8.1
			1	NE	ARG 1021 ARG	ionic		-4.3
			O1 1	NH2	1021 ARG 1021	ionic		-2.1
			O2 2	NE		ionic		-0.6
				NH2				-5.7
L24		-6.753	O2 2 O1 1	N	ASP 1046	H-acceptor	3.41 4.00	-2.5
				NZ	LYS 868	ionic		-0.5

Analysis of 21 samples showed that the GC chromatograms of all samples from the same species were qualitatively similar but differ by abundances of their major components. CA Performed from four discriminant compounds suggest the existence of two main clusters of *S. grandiflorus* essential oils (Figure 3).

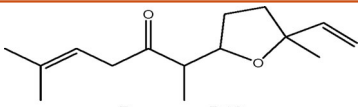
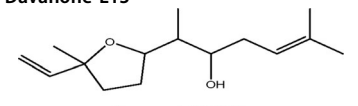
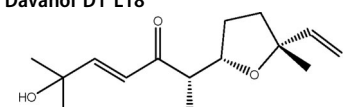
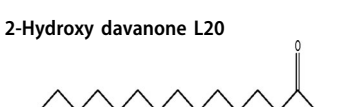
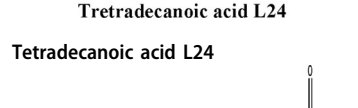
Group I (Y1–7) consisted mainly of oil samples dominated by 2-hydroxy davanone (4) (14.0–33.2%) and 5.5-dimethyl Furanone (5.5–9%). Whereas. Group II (Y8–Y21) includes oil samples

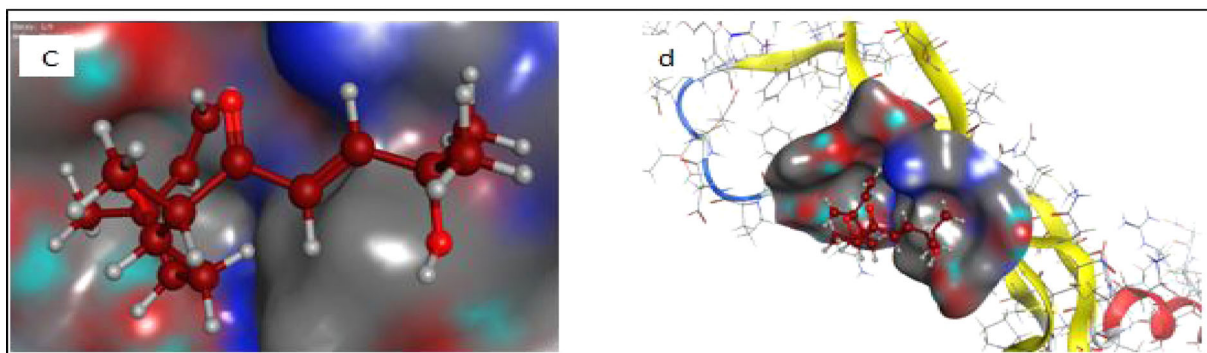
characterized by davanone (4) (41.3–73.2%), Davana ether (2) (0.7–5.3%) and hexadecanoic acid (3.2–16.8%; Figure 4, Table 1).

Cis-davanone has never been identified as up to 50% in essential oil of all species studied. The oils from stem parts of *Artemisia ciniformis* and *Artemisia kopetdaghensis* was the high percentage in all these species 40.1% and 47.9%, respectively. Davanoides are reported to have antifungal, antispasmodic and antibacterial properties. Indeed, the most compelling target among these was cis-hydroxy davanone,



**Table 4.** Results of energy balance of best complexes formed with anti-angiogenic drug molecules.

Targets	Chemical structure	Binding energy (Kcal/mole)	Rmsd -refine	Energy-conf	Energy- place	Energy- refine	RMSD
VEGF VEGFR-1 VEGFR-2	 Davanone L13	-3.992 -6.529 -4.778	1.454 1.338 1.1872	37.594 51.148 53.321	-29.409 -61.149 -54.385	-10.361 3.690 -8.944	1.417 1.237 1.053
VEGF VEGFR-1 VEGFR-2	 Davanol D1 L18	-3.811 -6.657 -6.657	2.0319 1.275 1.275	42.106 56.214 56.214	-28.2838 -65.602 -65.602	-9.492 -2.615 -2.615	1.397 1.278 1.278
VEGF VEGFR-1 VEGFR-2	 2-Hydroxy davanone L20	-4.066 -6.161 -3.391	1.343 1.716 1.533	17.758 21.885 35.967	-24.060 -52.651 -39.906	-9.659 -16.814 26.020	1.395 1.116 1.070
VEGF VEGFR-1 VEGFR-2	 Tetradecanoic acid L24	-3.809 -7.470 -6.753	0.958 1.327 1.187	-81.019 -76.820 -72.972	-38.265 -58.290 -66.076	-7.389 -18.760 -13.576	1.517 1.316 1.140
VEGF VEGFR-1 VEGFR-2	 Hexadecanoic acid L25	-4.0031 -8.504 -7.318	2.502 1.124 1.078	-79.796 -72.783 -69.892	-14.401 -58.660 -60.781	-9.407 -25.356 -8.456	1.560 1.219 1.011

**Figure 6.** The graphical illustration of interaction between (A) Davanone; (B) iso davanone; (C) The top scoring compound, d) A novel inhibitor L-20 identified by molecular docking 2- Hydroxydavanone was shown in the active site.

whose proved to have cytotoxic property (Hosseinzadeh et al., 2019). To our knowledge, there is only one study on the genus *Scolymus*. The main compounds of *S. hispanicus* were heneicosane (19.4%), hexahydro farnesly acetone (17.0%) and phytol (17.0%). However, no work was performed on chemical composition of essential oil of *S. grandiflorus* and this work is the first one (Servi, 2019).

The results showed important differences between the stations indicating the existence of chemical polymorphism. The observed differences in the chemical composition of

essential oils may be due to ecological factors or many other factors as to soil type's water stress and climatic conditions that influenced the plant (Belabbes et al., 2017).

### 3.3. Computational and theoretical approach

Enzymatic cavity with the residues of the active site for the three targets is shown in Figure 5. The ligands' of essential oils from the root of *S. grandiflorus* minimized toxicity and energy obtained by MOE software is shown in Table 2.

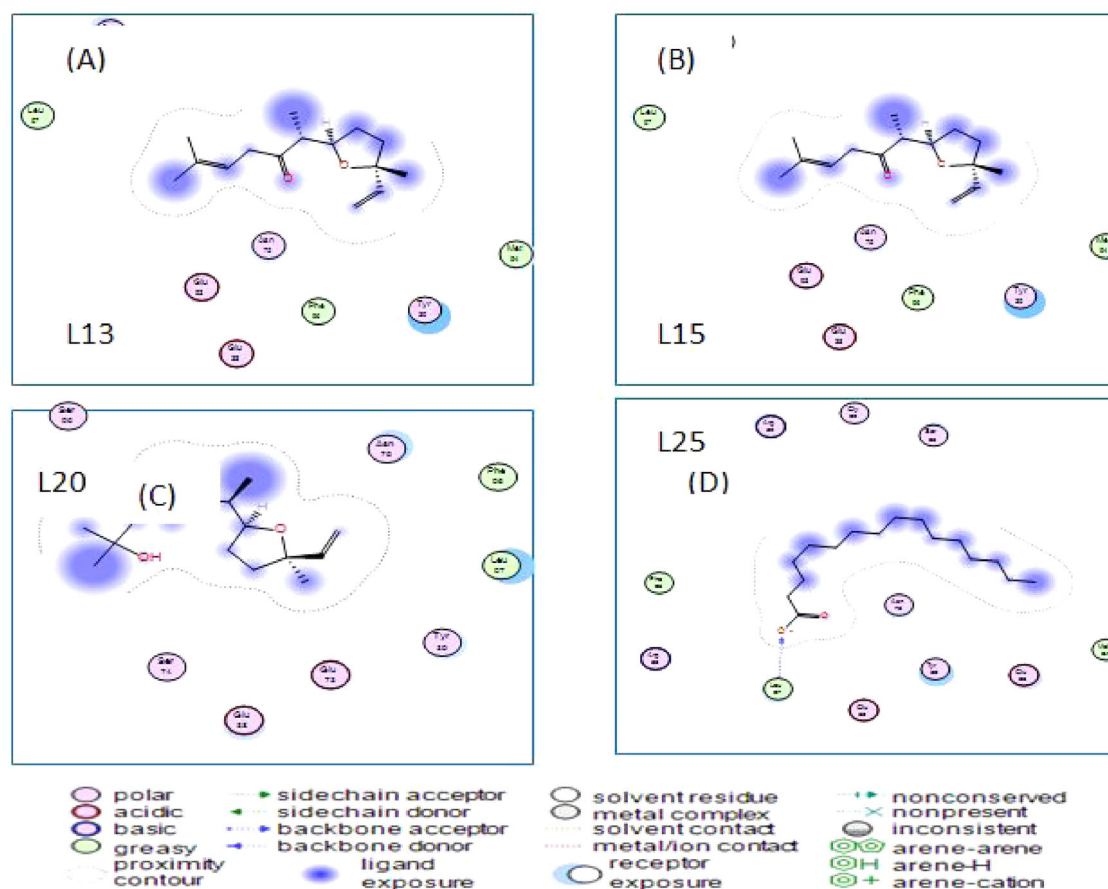


Figure 6 (Continued)

These ligands were capable of providing crucial biological activities in accordance with the principle of Lipinski et al. (1997) (Pettersson et al., 1988). As stated in the table above. We find that the molecules L13, L24 and L25 have a high value of Log P and Log S compared to other molecules and also the results obtained show that these ligands (L24, L13 and L25) have a high value of torsion angle relative to other compounds. This shows that these compounds were more flexible. As well, it is noted that the growth of the torsion angle depends on the binding number of the molecule.

### 3.4. Affinity of compounds with three targets

Results of docking calculations and bonds between atoms of best compounds and residues of the active site are given in Table 3. The results of bonds of the other compounds are given in Supporting Information Table 3(a).

### 3.5. Molecular docking analysis

#### 3.5.1. Interaction with VEGF

According to the results of Tables 3 and 4, out of the best compounds studied, 2-hydroxy davanone (Ligand 20; Figure 6) was predicted to be the strongest VEGF receptors binder that forms a complex with the most stability with the lowest energy  $-4.066$  Kcal/mol). The ligands that interact with VEGF were: Ligand L3 interacted with one amino acid LEU 97 at a distance of  $2.95$  Å strong with energy of  $-1.2$

and ligand L6 interacted with one amino acid GLU 38H-donor at a distance of  $3.08$  Å strong and energy binding of  $-2.0$ . Similarly, the ligand L24 interacted with two amino acids (LEU 97 and ARG 56) (H-acceptor, ionic) at a distance of  $2.82$  and  $3.99$  Å strong and low, respectively.

It is noted that the interactions between the residues of the active site of 5T89 and 2-hydroxy davanone ligand formed a stable complex. The second-best binder was hexadecanoic acid (Ligand 25) with the energy of  $4.0039$  Kcal/mol) that interacts with one amino acid LEU 97 H-acceptor at a distance of  $2.90$  Å strong interaction and energy binding of  $-2.8$  Kcal/mol. This suggests that hexadecanoic acid can inhibit VEGF receptors. Best ligand with VEGF is shown in Figure 6(a).

#### 3.5.2. Interaction with VEGFR-1

We note that hexadecanoic acid (Ligand 25; Figure 7) was predicted to be the strongest VEGF receptors binder that formed a complex with the most stability with the lowest energy  $-8.504$  Kcal/mol) that interacts with six amino acids (ARG 1021, ARG 1021) two H-acceptor and four ionic at a distance of  $3.00$ ,  $2.83$  and  $3.03$ ,  $3.45$ ,  $3.93$  and  $2.83$  Å strong, low, average interaction, with the existence of six electric force (GLU 910, GLU 878, CYS 912, LEU 882, ASP 1040 and LYS 861). The existence of electric force, suggesting that hexadecanoic acid can inhibit VEGF receptors. It is noted that the interactions between the residues of the active site of 3HNG and the hexadecanoic acid ligand formed a stable

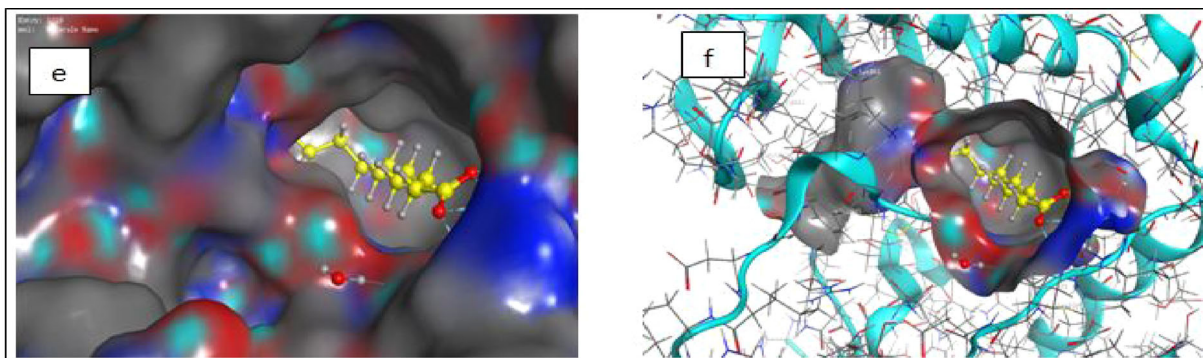


**Figure 7.** The graphical illustration of interaction between (A) iso davanone; (B) Tetradecanoic acid; (C) Hexadecanoic acid and (D) Davanol D1 with VEGFR-1. e) The top scoring compound f) A novel inhibitor L-25 identified by molecular docking Hexadecanoic acid was shown in the active site.

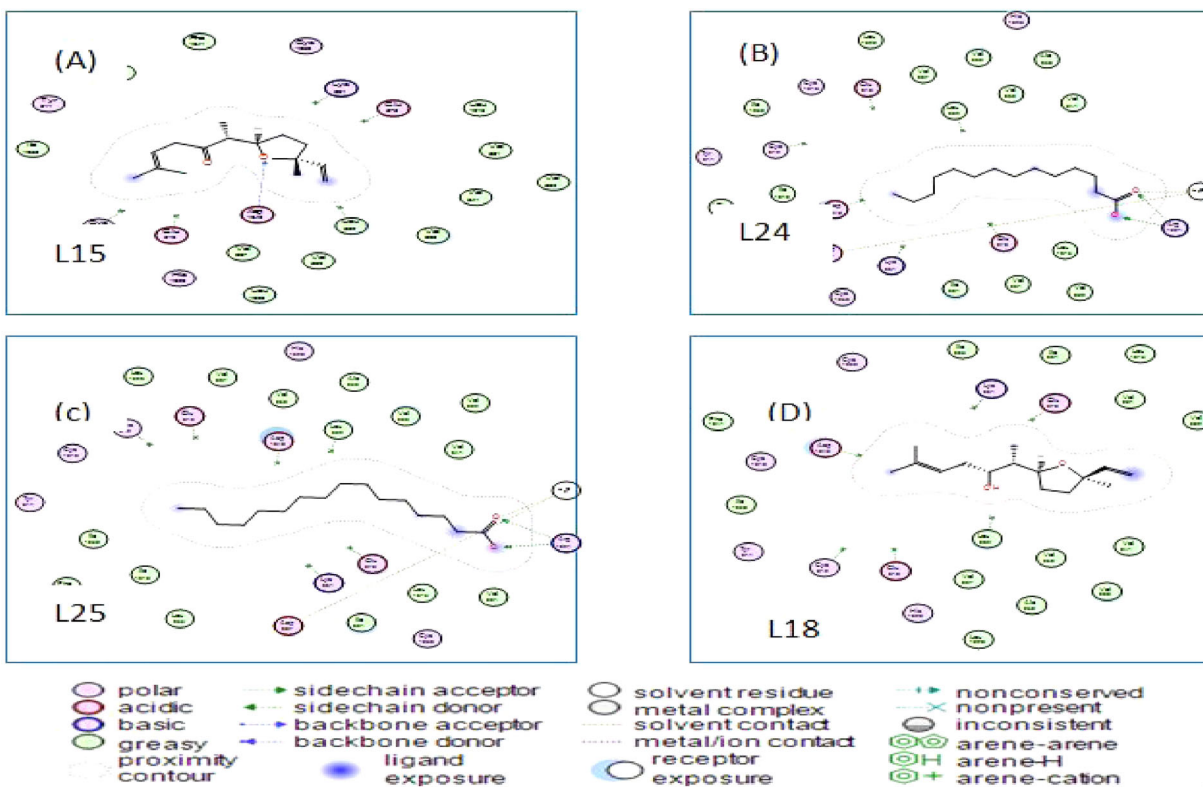


**Figure 7** (Continued)

complex with a strong interaction. Best ligand with VEGFR-1 is given in Figure 7(a).

### 3.5.3. Interaction with VEGFR-2

We note that hexadecanoic acid (Ligand 15; Figure 8) was predicted to be the strongest VEGF receptors binder that formed a complex with the most stability with the lowest energy  $-7.318$  Kcal/mol. The ligands that interact with VEGFR-2 were: Ligands L3, L5 and L6 interacted with one amino acid ASP 1046 and GLU 885 with H-acceptor and H-donor, respectively, at a distance of 2.98 and 2.58 Å low interaction with energy binding of  $-3.7$  and  $-2.8$  Kcal/mol. It is noted that the interactions between the residue of the active site of 2XIR and the hexadecanoic acid ligand formed a stable complex with a strong interaction.

The second best binder was tetradecanoic acid (Ligand 24) with the energy of  $-6.753$  Kcal/mol (Table 3), with the existence of two amino acids ASP 1046 and LYS 868 with H-acceptor and ionic at distance of 3.41 and 4.00, respectively, with energy binding of  $-2.5$  and  $-0.5$  Kcal/mol, respectively. Results of energy balance of best complexes formed with three targets are given in (Table 4). Energy for other compounds see best complexes formed Supporting Information Table 4(a). Best ligand with VEGFR-2 is given in Figure 8(a).

### 3.6. Interaction with ctDNA

Circulating tumor DNA (ctDNA) is a small fragment of DNA that found in the bloodstream of cancerous patients. Studies proposed that this tumor-based DNA fragment can act as a

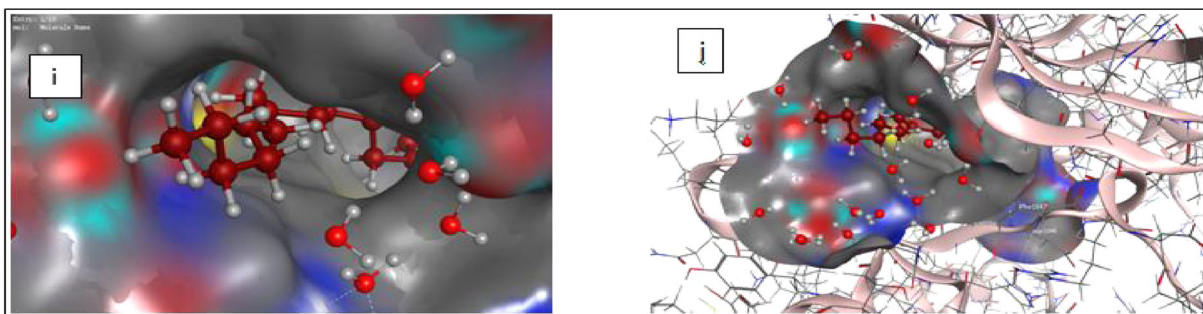


Figure 8. i) The top scoring compound, j) A novel inhibitor L-15 identified by molecular docking was Hexadecanoic acid was shown in the active site.

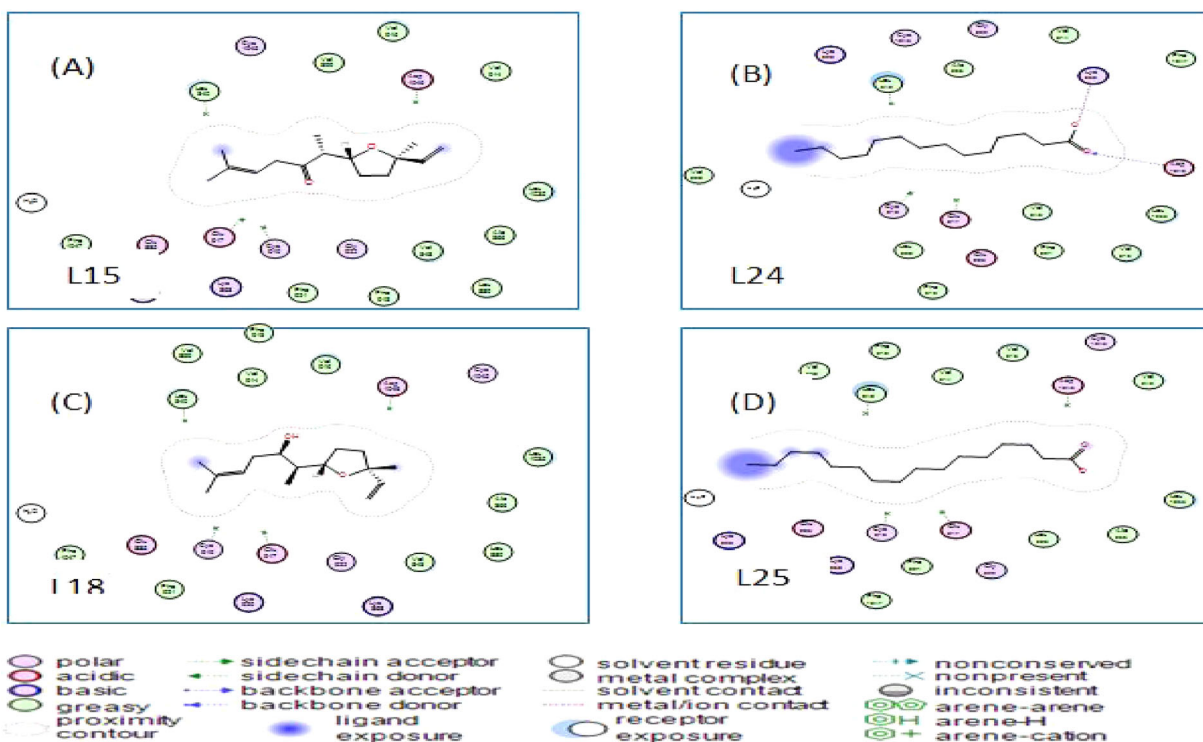


Figure 8 (Continued)

leader for the migration of tumor cells to other. Recently, this small fragment of DNA was considered as detectable biomarker in early- and late Stage human malignancies (Drach et al., 1996). A bioinformatic molecular docking study was carried out on ctDNA and is shown in (Table 5).

Our results demonstrated that the four compounds: hexadecanoic acid (Ligand 25), tetradecanoic acid (Ligand 24), davanone (Ligand 13) and davanol D1 (Ligand 18) were the best interacting compounds (Figure 9). The calculated docking energies for these compounds were, respectively,  $-7.210$ ,  $-6.984$ ,  $-6.223$  and  $-6.171$  Kcal/mol. With the exception of Lavender lactone, other compounds were located in the small cDNA groove. The docking simulation showed that Lavender lactone existed in the main groove region. The calculated docking energy for this compound was  $-4.191$  Kcal/mol (Table 4). From these results, it should be noted that several factors, notably the variability of the ligand structures and the capacity to build covalent and/or

noncovalent bonds, could affect their binding affinity to the small cDNA groove. There are even other factors such as the distribution of electrostatic charges with DNA and also the base pairs A: T (Neidle, 2001). Studies have suggested that minor groove binding ligands carry a cationic charge, complementing the potential in A: T regions. Our results are fully consistent with previous reports and the compounds studied interacted with A: T base pairs.

Figure 9 is replaced by another, from which we have assembled only the best ligands.

### 3.7. Interaction with VEGF-VEGFR

The two VEGF monomers participate in the interaction with the d2 domain of VEGFR1 (Figure 10). The results of docking energies of VEGF/VEGFR best inhibitors are shown in

(Table 6). The results of other compounds are shown in Supporting Information Table 6(a).

Numerous studies have shown that the VEGF gene is a key mediator of angiogenesis in cancer (Carmeliet, 2005). The VEGF protein is a homodimeric glycoprotein. Molecular docking results revealed that hexadecanoic acid, 2-Hydroxy davanone, davanone and iso davanone were the best compounds interacting with the suspected binding residues at the active VEGF site (see Supporting Information Figure 18).

**Table 5.** The docking energies of ctDNA inhibitors.

Compound	DE <sup>a</sup> (Kcal/mol)	ETOR (kT)	VDW (kT)	EIE (kT)
5,5-dimethyl Furanone	-5.053	278.718	336.166	-1550.53
Lavender lactone	-4.191	276.077	337.637	-1574.26
Cis-Arbusculon	-4.746	278.032	348.588	-1575.77
Trans-Arbusculon	-4.576	278.901	344.688	-1555.81
cis-Linalool oxide	-4.611	286.323	357.123	-1576.79
Davanafuran	-5.247	288.118	358.120	-1573.26
(E)- $\beta$ -Elemene	-5.022	281.461	363.974	-1578.91
Davana ether	-5.009	281.490	363.947	-1578.89
Davanone	-6.223	280.120	356.716	-1571.56
Iso davanone	-5.843	278.929	361.956	-1562.72
Davanol D1	-6.171	283.362	360.574	-1568.81
Eudesma-11-en-4 $\alpha$ -ol	-4.393	282.663	377.026	-1567.59
2-Hydroxy davanone	-5.884	280.596	335.328	-1550.61
Tetradecanoic acid	-6.984	257.680	349.569	-1562.28
Hexadecanoic acid	-7.210	255.039	349.577	-1564.55

<sup>a</sup>DE: Docking Energy; ETOR: torsion Energy; VDW: van der Waals; EIE: electrostatic interaction Energy.

The calculated docking energies for these molecules were, respectively,  $-4.003$ ,  $-4.066$ ,  $-3.992$  and  $-3.984$  Kcal/mol. Lavender lactone was the weakest interacting compound with this receptor. The calculated docking energy calculated for this compound was  $-3.251$  Kcal/mol, respectively. Also, among the anchored compounds, hexadecanoic acid, tetradecanoic acid, iso davanone and davanol D1 were the excellent compounds interacting with VEGFR-1 (see Supporting Information Figure 19). The calculated docking energies calculated for these compounds were, respectively,  $-8.504$ ,  $-7.470$ ,  $-6.534$  and  $-7.345$  Kcal/mol. Davana furan was the weakest compound with this receptor. The calculated docking energy calculated for this compound was  $-4.671$  Kcal/mol. Conforming to our molecular docking results, hexadecanoic acid, tetradecanoic acid, iso davanone and davanol D1 were the best compounds interacting with VEGFR-2 (see Supporting Information Figure 20). The calculated docking energies calculated for these compounds were, respectively,  $-7.318$ ,  $-6.753$ ,  $-4.780$  and  $-6.340$  Kcal/mol. With the exception of (E)- $\beta$ -Elemene, other compounds were found in the active site of VEGFR-2. The calculated docking energy observed for this compound was  $-3.314$  Kcal/mol. We observed that hexadecanoic acid showed a binding affinity for interacting with receptors for cDNA, VEGFR-1, VEGFR-2 and VEGF. Tetradecanoic acid interacted with cDNA, VEGFR-1 and VEGFR-2. In addition, davanol D1 has the affinity to interact with the cDNA of VEGFR-1 and VEGFR-2. Davanone

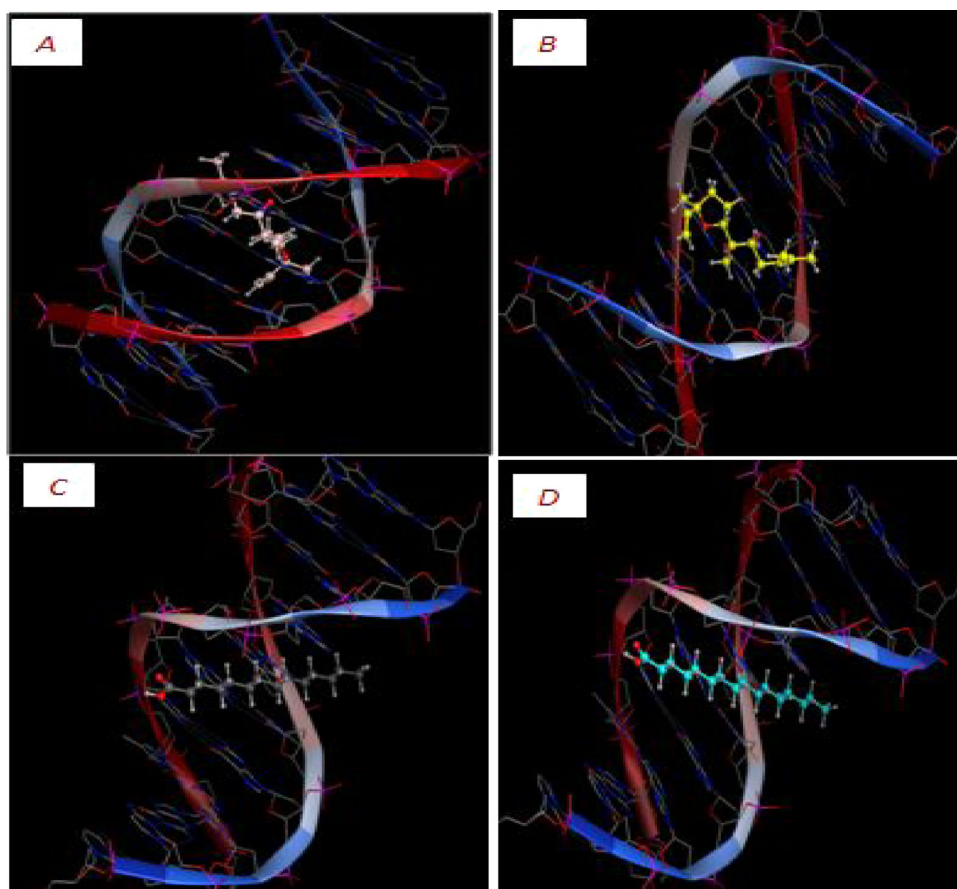


**Figure 9.** The graphical illustration of interaction between the four top docked compounds (A) davanone L13; (B) davanol D1 L18; (C) tetradecanoic acid L24 and (D) hexadecanoic acid L25 with ctDNA. The graphical illustration of interaction between the top docked compounds (A) Davanone L13; compound (B) hexadecanoic acid L25 with ctDNA.

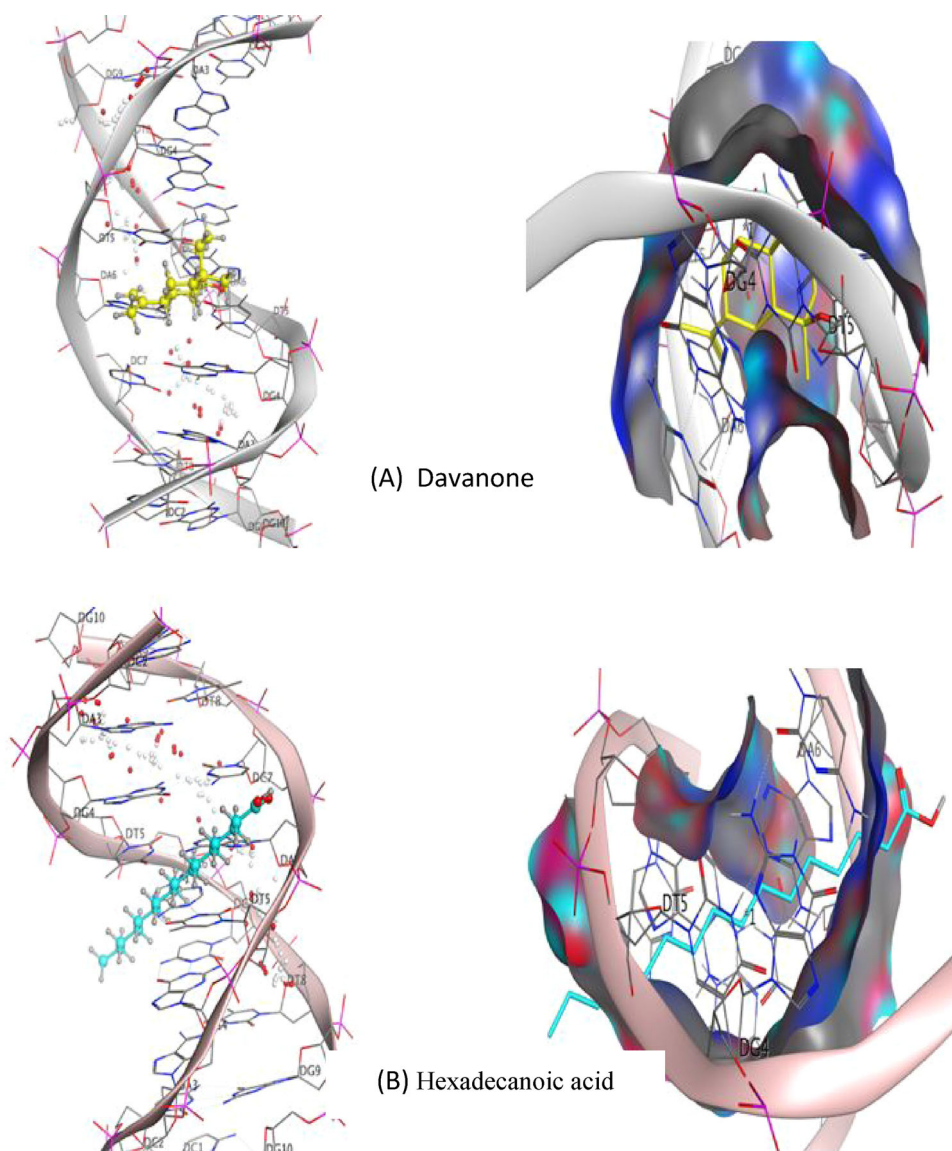


Figure 9. Continued

has the affinity to interact with cDNA and VEGF. Iso davanone has the affinity to interact VEGF of VEGFR-1 and VEGFR-2. 2-hydroxy davanone has the affinity to interact with only VEGF. Inhibiting the interaction between VEGF and VEGFR is an important way to prevent angiogenesis and the development of a malignant tumor in other tissues. The results given, we can conclude that the best inhibition this produced by two molecules hexadecanoic acid (Ligand L25) and davanone (Ligand L13).

### 3.8. MDs analysis

Thermodynamic properties using the MD simulation approach, we have studied the evolution thermodynamic properties of the ligands of complex 25 and 13 in NVT ensemble (Table 7).

The results represented in Table 7 revealed that the kinetic energies of translation and the internal energy for the L25 and L13 (for L13 see Supporting Information Figures

15–17) in the VEGF enzyme and the VEGFR1 receptor, were low compared to the VEGFR2 receptors, and the fluctuation in pressure for the VEGFR2 receptor was significant. Therefore, L13 and L25 were predicted to be the most interactive system. These results were in total agreement with the docking prediction results (see Tables 4 and 5). We can show the detailed analysis of MD simulation results of only compound L25 with target VEGF receptors to Figures 11–13.

### 3.9. *In silico* assessment of the ADME properties and drug-likeness

A computational study of best compounds was performed for the assessment of ADME properties (Table 8).

The ADME analysis of other compounds was shown in Supporting Information Table 8(a). The results exposed in Table 8 revealed that compounds (L13, L24 and L25) have high absorption. Also, we can note that these compounds comply with Lipinski's rule of 5, Veber's rule and Egan's rule.

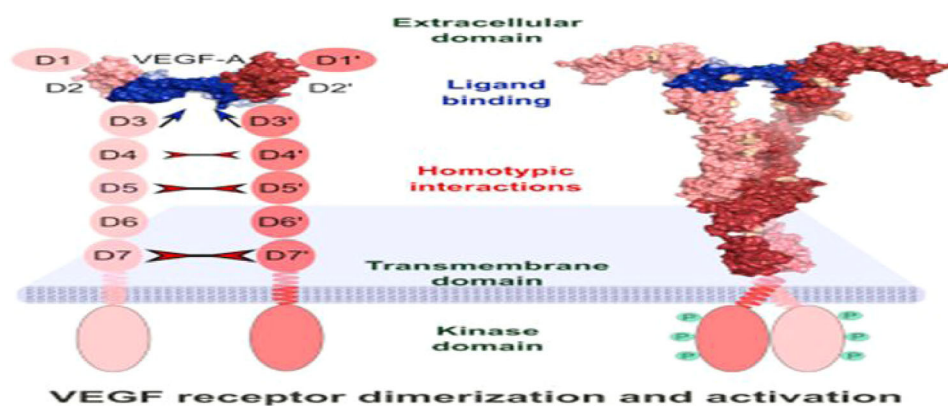


Figure 10. Structure of the VEGF receptor dimerization and activation in extracellular domain.

Table 6. The docking energies of VEGF/VEGFR inhibitors.

Compound	Receptor	DE			
		(Kcal/mol)	ETOR (kT)	EVDW (kT)	EIE (kT)
Davanone L13	VEGF	-3.992	435.552	1130.180	-2146.00
	VEGFR -1	-6.529	1348.713	4060.459	-7791.00
	VEGFR-2	-4.778	1408.056	6684.242	-16584.6
Davanol D1 L18	VEGF	-3.811	431.094	1113.038	-2086.24
	VEGFR -1	-7.345	1387.813	4085.864	-7713.85
	VEGFR-2	-6.340	1433.824	7013.454	-16721.3
2-Hydroxy davanone L20	VEGF	-4.066	432.167	1173.493	-2215.62
	VEGFR-1	-6.161	1384.406	3576.242	-7906.98
	VEGFR-2	-3.391	1410.636	7085.165	-16877.8
Tetradecanoic acid L24	VEGF	-3.809	415.596	1189.618	-2260.86
	VEGFR -1	-7.470	1353.340	4062.425	-7922.66
	VEGFR-2	-6.753	1367.229	6873.763	-16871.6
Hexadecanoic acid L25	VEGF	-4.003	388.611	1137.990	-2116.06
	VEGFR -1	-8.504	1378.607	4115.919	-7973.84
	VEGFR-2	-7.318	1411.548	7260.273	-16765.5

DE: docking energy; ETOR: torsion energy; VDW: van der Waals; EIE: electrostatic interaction energy.

Where  $\log P$  values ranged between (1.66. 3.69 and 4.19), respectively, ( $<5$ ), MW range (236.35. 228.37 and 256.42), respectively, ( $<500$ ), HBA range 3 – 2 and 2 ( $\leq 10$ ) and HBD range 1–1 and 1 ( $<5$ ), suggesting that these compounds would not be expected to cause problems with oral bioavailability, and thus, showing possible utility of both compounds for developing the compound with good drug like properties.

About the absorption parameters compounds L13, L20, L24, L18 and L25 present a promising oral availability, due to the optimal Caco-2 cell permeability and HIA ( $>0.9$  and  $>90\%$ , 197, respectively, Table 9) and skin permeability ( $\log K_p < -2.5$  for L24 and L25 (Table 9). Active components: L13-davanone, L20-(2-hydroxy davanone, L18-davanol D1, L24-tetradecanoic acid and L25-hexadecanoic acid. BBB: Blood-brain barrier. ADMET: Absorption. Distribution. Metabolism and Excretion and Toxicity. Minnow toxicity:  $< -0.3$ ; high acute toxicity, VDSS:  $< -0.15$  low,  $>0.45$  high, BBB:  $>0.3$  cross BBB,  $< -1$  poorly distributed to the BBB, CNS:  $> -2$  penetrate CNS,  $< -3$  unable to penetrate CNS, Low skin permeability:  $> -2.5$ , Caco-2 permeability:  $>0.9$ , Human intestinal absorption:  $>90$ . The overall lecture of (Table 9) highlights that compounds L13 could be excellent candidate as drugs. However, lead to further studies and manipulations. All compounds are not substrates of the renal

Table 7. Thermodynamic properties calculated in reels units. Pressure  $P = P^* \epsilon / \sigma^3$ .

SP <sub>i</sub>	Method	H	U	EKT	P
SPI	VEGR-Lig-13	0.3565	856.0253	1202.520	-52.263
	VEGR1-Lig-13	0.7526	1320.523	2542.023	-653.254
	VEGR2-Lig-13	1.0145	758.201	895.326	-45.2365
	VEGR-Lig-25	0.2105	850.2948	1141.135	346.096
	VEGR1-Lig-25	0.8368	1331.317	3419.039	-25.890
	VEGR2-Lig-25	0.8934	827.0451	1123.195	50.126

Energy of configuration  $U = U^* N\epsilon$ . Translation Kinetic Energy  $EKT = EKT^* N\epsilon$  and Enthalpy  $H = H^*$ .

organic cation transporter 2 (OCT2). All compounds passed the AMES tests. The volume of distribution (VDs) for our two best ligands L13 and L18 were, respectively, 0.199 and 0.033 suggest that the drug will be distributed in plasma since values of the VDss  $< -0.15$ . So, VDss describes the extent of drug distribution and the fraction unbound describes the portion of free drug in plasma that may extravasate. The compounds L13 and L18 may be interesting potential agents as a part of an anticancer therapy to relieve cancer-related pain.

The compounds reveal almost intermediate values of VDss. Molecule L20 was entirely unable to penetrate the central nervous system (CNS). Molecules L24 and L25 were unable to penetrate plasma or tissue and presented Minnow toxicity. The absorption and distribution parameters, respectively, have been graphically represented by the extended and renewed version of the Edan-Egg model named Brain Or Intestinal Estimated (BOILED) permeation predictive model (BOILED-Egg) (Figure 14). The Figure 14 showed that all ligands enter the brain by crossing the blood-cerebrospinal fluid barrier except L9. The BBB is a biological barrier that protects the brain from molecules that are toxic to the CNS (Central nervous system). Permeability of the BBB is employed for drug delivery to the brain (Jain, 2012). The blocking of active efflux transporters likep-glycoprotein (P-gp) is a method worn to get through the BBB.

Knowing that p-glycoprotein (P-gp) is localized in several tissues, such as the intestines, the kidneys, the liver, the immune system at the level of the blood-brain and placental barrier and has a great variability of substrates. The latter plays a role in the immune and hematological systems is still hypothetical. Moreover, it is involved in the transport of

**Table 8.** Lipinski's rule of five for ADME analysis of best inhibitors (ligands).

N°	Name	Lipinski's rule of five				No. of rule violations Less than 2 Violations	Drug-likeness Lipinski's rule follows
		Molecularweight (g/mol) Less than 500 Dalton	Lipophilicity (MLogP) Less than 5	Hydrogen bond donors Less than 5	Hydrogen bond acceptors Less than 10		
13	Davanone	236.35	2.54	0	2	0 violation	Yes
18	Davanol D1	238.37	2.63	1	2	0 violation	Yes
20	2-Hydroxy davanone	252.35	1.66	1	3	0 violation	Yes
24	Tetradecanoic acid	228.37	3.69	1	2	0 violation	Yes
25	Hexadecanoic acid	256.42	4.19	1	2	1 violation: MLOGP > 4.15	Yes

MW: molecular weight; MLogP: logarithm of partition coefficient of the compound between water and n-octanol: n-OHND: number of hydrogen bonds donors; n-ON acceptors: number of hydrogen bond acceptors; n-ROTB: number of rotatable bonds.

**Table 9.** Pharmacokinetic and toxicity evaluated parameters of best compounds.

		13	20	18	24	25
Absorption	Human intestinal	96.829	95.234	93.407	92.691	92.004
	Skin permeability	-2.269	-3.169	-2.286	-2.705	-2.717
	Caco-2 permeability	1.366	1.337	1.638	1.56	1.558
Distribution	Surface area	104.738	109.533	109.533	100.439	113.169
	VDss (human)	0.199	0.033	0.23	-0.578	-0.543
	Fraction unbound (human)	0.385	0.476	0.401	0.171	0.101
	BBB permeability	0.553	-0.189	0.544	-0.027	-0.111
	CNS permeability	-2.684	-3.091	-2.841	-1.925	-1.816
Excretion	Total clearance	1.512	1.432	1.494	1.693	1.763
	Renal organic cation transporter	No	No	No	No	No
Toxicity	Oral rat acute toxicity (LD50)	1.997	1.995	1.853		1.44
	AMES toxicity	No	No	No	No	No
	Tetrahymena Pyriformis toxicity	1.265	0.995	1.499	0.978	0.84
	Min now toxicity	0.979	1.794	1.241	-0.601	-1.083

green = good, yellow = tolerable msmoh, red = bad. tdkhol.

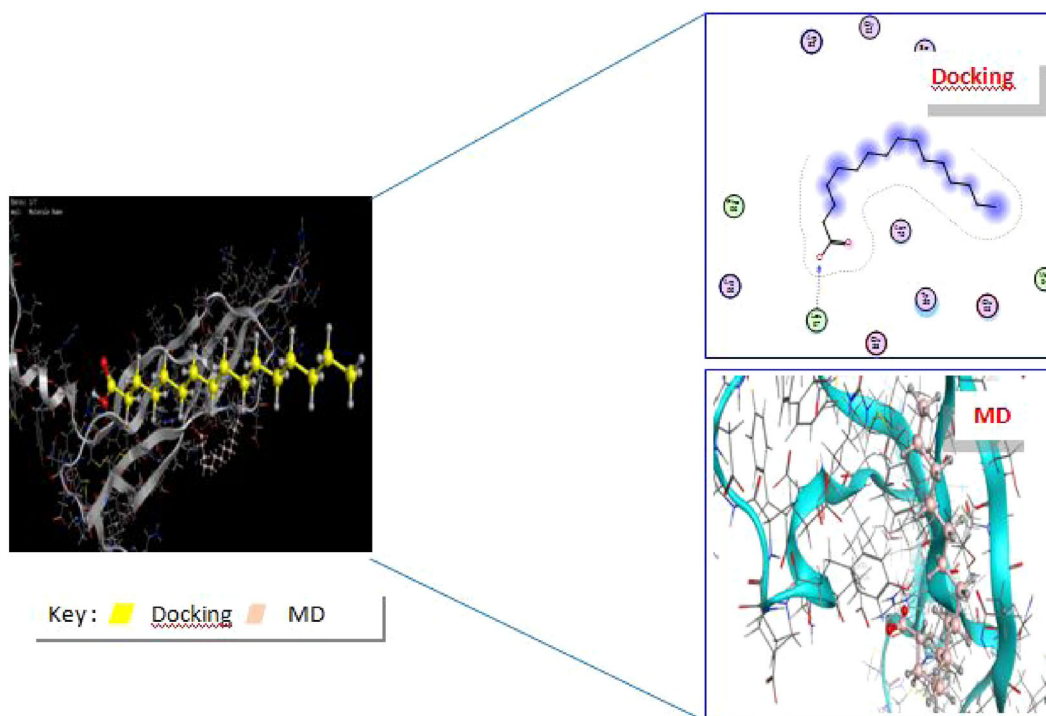


**Figure 11.** The compound – 25 hexadecanoic acid was docked without water well into the binding site of VEGF and has the highest dock score; there was also a clear difference between the final ligand pose and the docking pose after a molecular dynamics (MD) simulation.

certain interleukins and gamma interferon, as well as in the protection of stem cells against endogenous compounds and xenobiotics (Mesli & Bouchentouf, 2019). So, it is very effective to know their influences on the nervous system since their substrates are probably to change pharmacokinetics.

All molecule (P-gpsubstrate: No) were not predicted to be effluated from central nervous system by g-glycoprotein. So, it is preferable to choose L13 (davanone) to both VEGF (Vascular Endothelial Growth Factor)/VEGFR interaction to other ligands because L13 (davanone) have potent binding



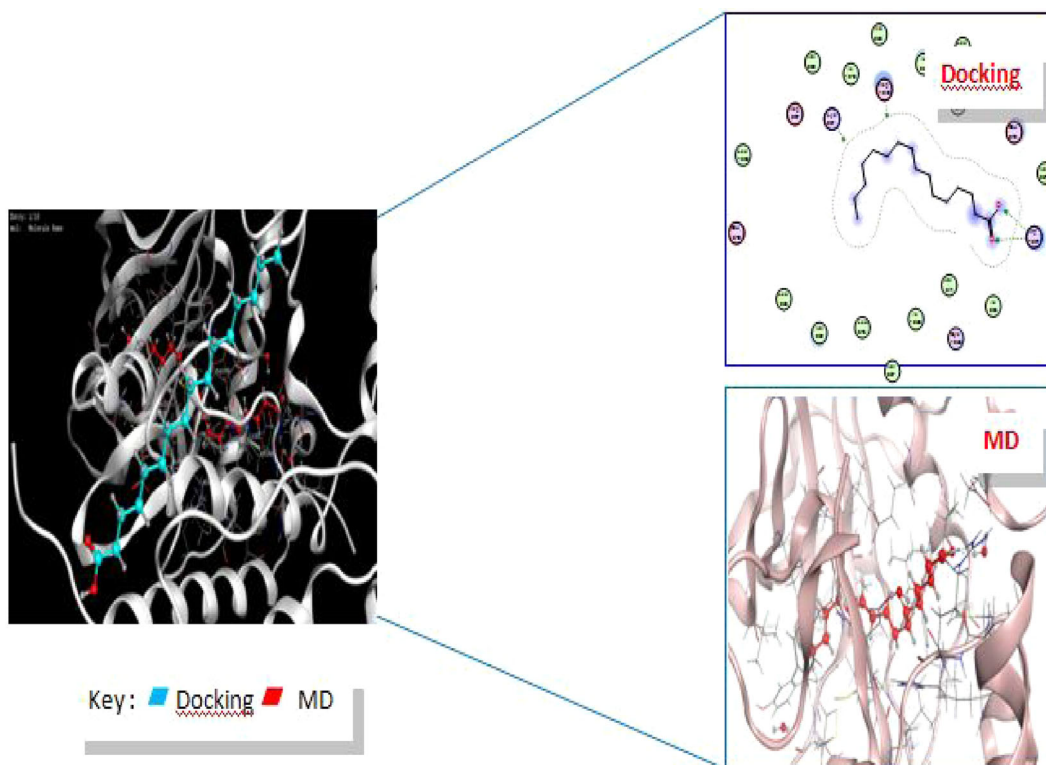


**Figure 12.** The compound – 25 hexadecanoic acid is docked without water well into the binding site of VEGFR-1 and has the highest dock score; there was also a clear difference between the final ligand pose and the docking pose after a MD simulation.

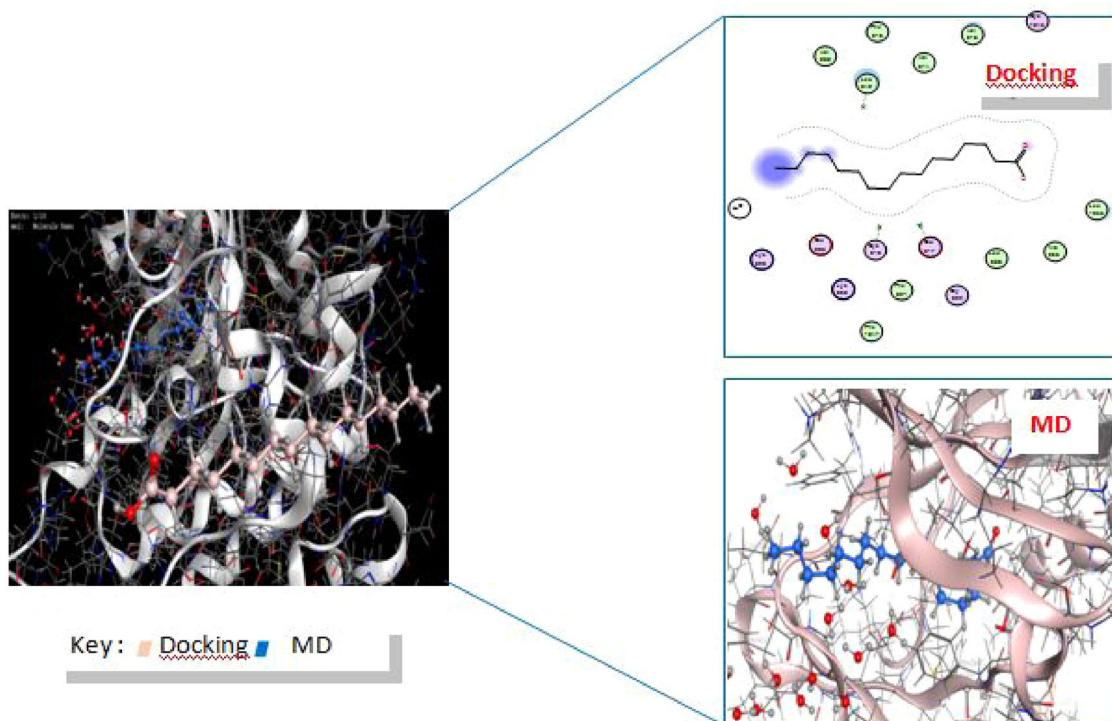


**Figure 13.** The compound – 25 hexadecanoic acid is docked without water well into the binding site of VEGFR-2 and has the highest dock score; there was also a clear difference between the final ligand pose and the docking pose after a MD simulation.

affinities, (L13 was not predicted to be effluated from central nervous system by g-glycoprotein). The ADMET properties and BOILED-Egg (Figure 14) plot validate the compound 13 and 18 pass the brain barrier and have high absorption in the intestines with good bioavailability. Compound 13

(davanone) has the highest binding affinity among all the inhibitors, it is proposed as a natural orally active drug. By analyzing the drug's score (*S*-value), davanone ligand 13 showed the lowest *S*-value –6.223 Kcal/mol with ctDNA for VEGF (Vascular Endothelial Growth Factor)/VEGFR interaction,

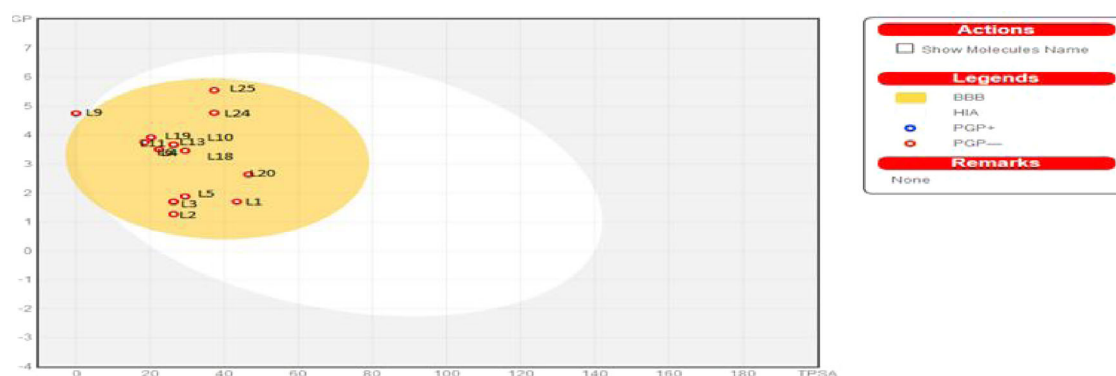


**Figure 14.** BOILED-Egg plot. Points located in the BOILED-Egg's yolk (yellow) represent the molecules predicted to passively permeate through the BBB. Whereas the ones in the egg white were relative to the molecules predicted to be passively absorbed by the gastrointestinal tract; the blue dots indicate the molecules for which it was expected to be effluated from the central nervous system (CNS) by the P-glycoprotein. Whereas the red ones point-out to the molecules predicted not to be effluated from the CNS by the P-glycoprotein.

**Table 10.** Drug-likeness, lead-likeness and PAINS parameters of best compounds.

MNP ID		L13	L20	L18	L24	L25
Drug-likeness	Lipinski violations	0	0	0	0	1
	Ghose violations	0	0	0	0	1
	Veber violations	0	0	0	1	1
	Egan violations	0	0	0	0	1
	Muegge violations	0	0	0	1	2
Lead-likeness violations	1	0	2	3	2	
PAINS alerts	0	0	0	0	0	

resulting as the best ligand among our selected ligands to block tumor growth without inducing too many side effects. So, ligand 13 (davanone) was proposed to be a potential therapeutic inhibitor of VEGF/VEGFR interaction. In this study, Ligand 18 (davanol D1) reveals the lowest Score of  $-6.171$  Kcal/mol with ctDNA was predicted as the second-best target inhibitor (with maximum binding affinity for VEGF/VEGFR interaction after L13).

In addition to the Lipinski rule of five, other four drug-likeness rules named Ghose, Egan, Veber and Muegee, have been contemporarily satisfied by compound L13 with the exception of molecule L24 and L25 (Table 10). Instead, the stringent lead-like criteria of Teague have been passed by compounds L13. Since lead-likeness tests were intended to provide leads with high affinity in high-throughput screens that allow for the discovery and exploitation of additional interactions in the lead-optimization phase, molecule L13 was excellent candidate to be investigated based on scaffold hopping approach. Finally, the outcome of the pan assay interference structures (PAINS) model, conceived to exclude small molecules that are likely to show false positives in biological assays, post no alert for the compound L13, concerning the presence of a molecule moiety.

### 3.10. Pharmacokinetics and medicinal chemistry properties

The results Medicinal Chemistry and Pharmacokinetics revealed that all compounds have High GI absorptions. We notice that there was a complement between our results for assessment of ADME properties (Table 9) and the predicted

results in medicinal chemistry and pharmacokinetics (Table 11).

Davanone of essential oils of the root of the *S. grandiflorus* (Ligand 13) was predicted to be characterized by a high lipophilicity and high coefficient of skin permeability  $\log K_p$  by providing hexadecanoic acid (Ligand 25) and 2-hydroxy davanone (Ligand 20). We can explain that the more negative the  $\log K_p$  (with  $K_p$  in cm/s), the less the molecule was absorptive to the skin, which explains the reliability of our study. We cite the works which have valid the stability of complexes and their affinities by MOE software (Mesli & Bouchentouf, 2019; Mesli et al., 2019).  $\log Po/w L25 > \log Po/w L18 > \log Po/w L13$ . So, Ligand L13 represents high affinity with VEGF receptors. Synthetic accessibility (SA) was a major factor to take into account in this selection process an acceptable value between 3.96, 4.27 and 2.31 for the ligands (L13, L18 and L25), respectively, these are more encouraging compounds which can be synthesized or subjected to bioassays or other experiments. Our previous research has revealed that oils from our region have better biological activities (Benyoucef et al., 2020; Drach et al., 1996). Validation of our results, for essential oils of the *S. grandiflorus* immunotherapy (Clinic) is mentioned in (Table 12). These four (4) molecules (Afinib, Erlotinib, Gefitinib, Osimertinib) prevent tumor growth by inhibiting the action of EGFR, a protein that sends a division signal to the cell. Unfortunately, they have side effects, and therefore, the main anti-angiogenic agent administered is the Bevacizumab a monoclonal antibody (non-small cell lung cancer). Sunitinib blocks the tyrosine kinase activities of vascular endothelial growth factor receptor 2 (VEGFR2), is an oral small-molecule, multitargeted receptor tyrosine kinase (RTK) inhibitor.

Regorafenib is an orally bioavailable small molecule with potential anti-angiogenic and antineoplastic activities. There are even checkpoint inhibitors which are monoclonal antibodies but they have a different action, which is why they are classified as specific immunotherapies. The goal of which is to restore an immune response that allows the immune system to attack abnormal elements. The goal is to find a natural inhibitor molecule with no side effects. Our molecular docking results with ctDNA coincided with clinical results; the oxygenated compounds were the most dominant with a

**Table 11.** Pharmacokinetics and Medicinal Chemistry properties for best molecule.

Molecule	Pharmacokinetics		Medicinal Chemistry	
	GI absorption	Log $K_p$ (skin permeation)	Lead likeness	Synthetic accessibility
Davanone L13	High	-5.38 cm/s	No; 1 violation: MW < 250	3.96
Davanol D1 L18	High	-5.17 cm/s	No; 2 violations: MW < 250, XLOGP3 > 3.5	4.27
2-Hydroxy davanone L20	High	-6.50 cm/s	Yes Pains; o alert Brenk:2 alerts: isolated_alkene. michael_acceptor_1	4.04
Tetradecanoic acid L24	High	-3.35 cm/s	No; 3 violations: MW < 250. Rotors > 7. XLOGP3 > 3.5	2.09
Hexadecanoic acid L25	High	-2.77 cm/s	No; 2 violations: Rotors > 7. XLOGP3 > 3.5	2.31

**Table 12.** Energy balance of complexes formed with ctDNA under other clinical and our results for essential oils of the *S. grandiflorus*.

Drugs	ctDNA	Voie
<b>Immunotherapy (Clinic)</b>		
<b>Lung cancer</b>		
Afatinib	-8.630	Injectable
Gefitinib	-8.365	orally at a pre determine dose daily
Erlotinib	-7.481	Injectable
Osimertinib	-7.811	orally at a pre determine dose daily
<b>Kidney cancer</b>		
Sunitinib	-8.019	Oral
<b>Liver cancer</b>		
Regorafenib	-8.578	Oral
<b>Our Results</b>		
Davanone Lig13	-6.223	Oral
Hexadecanoic acid Lig25	-7.210	Oral

percentage 76.6–97.2%. Our ligand natural, hexadecanoic acid L25 (13.2%) better stabilized the system with its energy of -7.210 Kcal/mol, we compared with the components of Immunotherapy Clinic (see Table 12). The latter presents violations and toxicity, it cannot be presented as the best ligand, but davanone (Ligand13) with energy binding of -6.223 Kcal/mol could be excellent candidate as drugs because represents better the absorption 96.829 (see Table 8) among others ligands and the volume of distribution (VDss) suggest that the drug will be distributed in plasma. Moreover, the latter does not represent any violation (see Table 9) by contribution to the other ligands and again from the Table 10. Davanone was characterized by a high lipophilicity and high coefficient of skin permeability log  $K_p$ . Therefore, we propose ligand 13 as the best ligand which allows the inhibition of Vascular Endothelial Growth Factor receptors (VEGFR) and in the meantime, we suggest Ligand L13 davanone presented in essential oils of the root of the *S. grandiflorus* with its validated activity Score (-3.992, -6.529 and -4.778), respectively, for (VEGF, VEGFR-1 and VEGFR-2) as a new oral ligand despite obeying Lipinski's rule.

The present bioinformatic analysis MDs simulations were used to scrutinize novel oxygenated sesquiterpenes as inhibitor of Vascular Endothelial Growth Factor receptors (VEGFR). Preceding studies has indicated that davanone has been shown to have antitumor activity *in vitro*, many studies were focused on the inhibitory effect of the (*Eugenia jambolana*, *Musa paradisiaca* and *Coccinia indica*) extracts and date palm pollen (DPP), to key enzymes linked to cancer therapy, vascular endothelial growth factor receptors (Rasouli et al., 2018).

The  $IC_{50}$  value calculated for the hydro-alcoholic extract of (DDP) examined in the angiogenesis model was 260  $\mu$ g/mL. The results showed a decrease in the proliferation of endothelial cells. The results showed that the expression of the VEGF, MMP-2 and MMP-9 genes was significantly low. Harsha

Raj et al. (2017), we proved that the molecule from EA extracts of *E. Jambolana* and *M. Paradisiacal* can be developed into anticancer drugs. EA extracts of *E. Jambolana* and *M. paradisiacal* exhibited the highest cytotoxicity ( $IC_{50} = 25$  and 60 L g/mL), inhibited cell proliferation (up to 81%). The same acid that we have validated (*N*-hexadecanoic acid) has proven to be of major interest in previous research. This molecule extract from the leaves of *Kigelia pinnata* showed significant cytotoxicity against human colorectal carcinoma cells (HCT-116) with an  $IC_{50}$  value of 0.8  $\mu$ g/mL (Ravi & Krishnan, 2016). The researches of Mansoor et al we have shown that always our best validated molecule (*N*-hexadecanoic acid) proved its anticancer effect (Saljooghianpour & Javaran, 2013). The study of Hosseinzadeh et al. (2019) we have exposed that sesquiterpenoids (hydroperoxide of davanone (1) and hydroxy davanone (2)) were identified as the active constituents responsible for the cytotoxic property of the petroleum ether extract of *A. aucheri*. This research has shown that 24h treatment with  $IC_{50}$  concentration of compound 2 increased caspase-3 activation in A2780 and MCF-7 cell lines and compounds 1 increased activity of caspase 3 in A2780 and SK-N-MC cell lines, between these compounds, compound 1 exhibited more potent activity against the MCF-7, SK-N-MC and A2780 cell lines with  $IC_{50}$  values of  $8.45 \pm 0.81 \mu$ g/mL,  $9.60 \pm 1.32 \mu$ g/mL and  $10.9 \pm 2.03 \mu$ g/mL in A2780, MCF-7 and SK-N-MC cells, respectively. Compound 1 inhibited the growth of human cancer cells by induction of apoptosis (Hosseinzadeh et al., 2019). In our research the software package (MOE) does not detect any mark of the hydrophobic interactions between davanone and both the Vascular Endothelial Growth Factor receptors; what may be connected to the large size of this compound and the high number of torsion angles. The results were identified to have inhibitory activities against novel cDNA, VEGF and its receptors. Of these ligands, davanone (Ligand 13) has a stronger bond and high absorption in the intestines with good bio-availability. Therefore, the study carried out in this research reveals many secrets conveyed by the use of magic plants. Currently, herbal medicine offers solutions to heal with plants. It is a solution that is both alternative and complementary to the treatments of classical medicine, which are more and more popular and whose effectiveness is increasingly recognized.

#### 4. Conclusion

In conclusion, the results showed that plant is a good source of davana derivatives and oxygenated components. The chemical composition of *S. grandiflorus* essential oil showed

a significant variability. Results showed the positive correlations between the amounts of components and altitude. The inhibition of Vascular Endothelial Growth Factor receptors was theoretically investigated by two methods of computational chemistry: molecular docking analyzes MD simulations, ADME properties and pharmacological knowledge. Our ligand and natural inhibitor davanone has an affinity to interact with cDNA, VEGF and its receptors. This model showed a significant decrease of energy (score) and there by an increase of the inhibition activity. However, the combination between docking simulation and MD simulations proved the stability of the complex formed by ligand L13. Although two compounds L13 and L25 have potent binding affinity with VEGF receptors in the docking simulation. Moreover, the ADMET properties and BOILED-Egg plot validated the compound 13 and 25 that passed the brain barrier and have high absorption in the intestines with good bioavailability. Davanone has the highest binding affinity among all the inhibitors, it is proposed as a natural orally active drug and reliable treatment during the first stage of cancerous cells.

### Ethics approval and consent to participate

Not applicable.

### Consent For publication

Not applicable.

### Funding

None.

### Disclosure statement

No potential conflict of interest was reported by the authors.

### Acknowledgement

Authors thanks the Algerian Ministry of Higher Education and Scientific Research for the support under the PRFU project (approval No. B00L01UN130120190009) and (approval No. B00L01UN130120180004).

### ORCID

Mohammed Semaoui  <http://orcid.org/0000-0003-2768-306X>

### References

Al-Hader, A., Aqel, M., & Hasan, Z. (1993). Hypoglycemic effects of the volatile oil of *Nigella sativa* seeds. *International Journal of Pharmacognosy*, 31(2), 96–100. <https://doi.org/10.3109/13880209309082925>

Alwahibi, L. H., Abdel-Mageed, W. M., Abdelkader, M. S., Bayoumi, S., Basudan, O., El-Gamal, A. A., & Bolla, K. (2016). Sesquiterpene lactones and flavonoids from *Artemisia sieberi*. *International Journal of Pharmacognosy and Phytochemical Research*, 8(4), 639–644.

Bekhechi, C., Boti, J. B., Bekkara, F. A., Abdouahid, D. E., Casanova, J., & Tomi, F. (2010). Isothymo in Ajowan essential oil. *Natural Product Communications*, 5(7), 1107–1110.

Belabbes, R., Dib, M. E. A., Djabou, N., Ilias, F., Tabti, B., Costa, J., & Muselli, A. (2017). Chemical variability, antioxidant and antifungal activities of essential oils and hydrosol extract of *Calendula arvensis* L. from western Algeria. *Chemistry & Biodiverse*, 14(5), e1600482.

Benyoucef, F., Dib, M. E. A., Tabti, B., Zoheir, A., Costa, J., & Muselli, A. (2020). Synergistic effects of essential oils of *Ammoides verticillata* and *Satureja candidissima* against many pathogenic microorganisms. *Anti-Infective Agents*, 18(1), 72–78. <https://doi.org/10.2174/2211352517666190227161811>

Berendsen, H. J., Postma, J. V., van Gunsteren, W. F., DiNola, A. R. H. J., & Haak, J. R. (1984). Molecular dynamics with coupling to an external bath. *Journal of Computational Physics*, 81(8), 3684–3690.

Bond, S. D., Leimkuhler, B. J., & Laird, B. B. (1999). The Nosé–Poincaré method for constant temperature molecular dynamics. *Journal of Computational Physics*, 151(1), 114–134. <https://doi.org/10.1006/jcp.1998.6171>

Bouzabata, A., Boussaha, F., Casanova, J., & Tomi, F. (2010). Composition and chemical variability of leaf oil of *Myrtus communis* from north-eastern Algeria. *Natural Product Communications*, 5(10), 1659–1662.

Carmeliet, P. (2005). VEGF as a key mediator of angiogenesis in cancer. *Oncology*, 69(3), 4–10. <https://doi.org/10.1159/000088478>

Chakraborty, S., & Rahman, T. (2012). *The difficulties in cancer treatment* (Vol. 6, 16th ed.). Ecancermedalscience. <https://doi.org/10.3332/ecancer2012.ed16>

Conseil de l'Europe. (1996). *Pharmacopée Européenne, Maisonneuve S.A. Sainte Ruffine*.

Daoud, I., Melkemi, N., Salah, T., & Ghalem, S. (2018). Combined QSAR, molecular docking and molecular dynamics study on new Acetylcholinesterase and Butyrylcholinesterase inhibitors. *Computational Biology and Chemistry*, 74, 304–326. <https://doi.org/10.1016/j.compbiolchem.2018.03.021>

Desfontaines, R. L. (1800). *Flora Atlantica Sive Historia Plantarum, Quae in Atlante, Agro Tunetano et Algeriensi Crescunt*, 2. *Missouri Botanical Garden's Rare Books Collection*, 1–458. <https://doi.org/10.5962/bhl.title.323>

Drach, J., Gsur, A., Hamilton, G., Zhao, S., Angerler, J., Fiegl, M., Zojer, N., Raderer, M., Haberl, I., Andreeff, M., & Huber, H. (1996). Involvement of P-glycoprotein in the transmembrane transport of interleukin-2 (IL-2), IL-4, and interferon-gamma in normal human T lymphocytes. *Blood*, 88(5), 1747–1754. <https://doi.org/10.1182/blood.V88.5.1747.1747>

El Baroty, G. S., Goda, H. M., Khalifa, E. A., & Abd El Baky, H. H. (2014). Antimicrobial and antioxidant activities of leaves and flowers essential oils of Egyptian *Lantana camara* L. *Der Pharma Chemica*, 6, 246–255.

Esselin, H., Soutour, S., Liberal, J., Cruz, M. T., Salgueiro, L., Siegler, B., Freuze, I., Castola, V., Paoli, M., Bighelli, A., & Tomi, F. (2017). Chemical composition of *Laurencia obtusa* extract and isolation of a new C15-acetogenin. *Molecules*, 22(5), 779. <https://doi.org/10.3390/molecules22050779>

Ghufran, M., Rehman, A. U., Shah, M., Ayaz, M., HO, H. L., & Wadood, A. (2019). In-silico design of peptide inhibitors of K-Ras target in cancer disease. *Journal of Biomolecular Structure and Dynamics*, 38(18), 5488–5499. <https://doi.org/10.1080/07391102.2019.1704880>

Guarrera, P. M., & Savo, V. (2016). Wild food plants used in traditional vegetable mixtures in Italy. *Journal of Ethnopharmacology*, 185, 202–234. <https://doi.org/10.1016/j.jep.2016.02.050>

Halgren, T. A. (1996). Merck molecular force field. I. Basis, form, scope, parameterization, and performance of MMFF94. *Journal of Computational Chemistry*, 17(5–6), 490–519. [https://doi.org/10.1002/\(SICI\)1096-987X\(199604\)17:5/6<490::AID-JCC1>3.0.CO;2-P](https://doi.org/10.1002/(SICI)1096-987X(199604)17:5/6<490::AID-JCC1>3.0.CO;2-P)

Halgren, T. A. (1999). MMFF VII. Characterization of MMFF94, MMFF94s, and other widely available force fields for conformational energies and for intermolecular-interaction energies and geometries. *Journal of Computational Chemistry*, 20(7), 730–748. [https://doi.org/10.1002/\(SICI\)1096-987X\(199905\)20:7<730::AID-JCC8>3.0.CO;2-T](https://doi.org/10.1002/(SICI)1096-987X(199905)20:7<730::AID-JCC8>3.0.CO;2-T)

Harsha Raj, M., Ghosh, D., Banerjee, R., & Salimath, B. P. (2017). Suppression of VEGF-induced angiogenesis and tumor growth by *Eugenia jambolana*, *Musa paradisiaca*, and *Cocciniaindica* extracts. *Pharmaceutical Biology*, 55(1), 1489.

Hosseinzadeh, L., Shokoohinia, Y., Arab, M., Allahyari, E., & Mojarrab, M. (2019). Cytotoxic and apoptogenic sesquiterpenoids from the

- petroleum ether extract of *Artemisia aucheri* aerial parts. *Iranian Journal of Pharmaceutical Research*, 18(1), 391–399.
- Jain, K. K. (2012). *Blood–brain barrier*. MedLink Neurology.
- Markovic-Mueller, S., Stutfeld, E., Asthana, M., Weinert, T., Bliven, S., Goldie, K. N., Markovic-Mueller, S., Stutfeld, E., Asthana, M., Weinert, T., Bliven, S., Goldie, K. N., Kisko, K., Capitani, G., & Ballmer-Hofer, K. (2017). Structure of the full-length VEGFR-1 extracellular domain in complex with VEGF-A. *Structure (London, England: 1993)*, 25(2), 341–352. <https://doi.org/10.1016/j.str.2016.12.012>
- Marrone, T., Hu-Lowe, D., Grazzini, M., Yin, M. J., Chen, J., Hallin, M., Amundson, K., Yamazaki, S., Romero, D., McHarg, A., Blasi, E., Hong, Y., Tompkins, E., Palmer, C., Deal, J., Murray, B., Solowiej, J., McTigue, M., Wickersham, J., & Bender, S. (2007). PF-00337210, a potent, selective and orally bioavailable small molecule inhibitor of VEGFR-2. *American Association for Cancer Research*, 67(9), 3992.
- Martin, F. W., & Ruperté, R. M. (1979). *Edible leaves of the tropics*. US Dep. Agric. Sci. Edu. Admin., Agric. Res., Southern Region, Mayagüez, PR.
- Medbouhi, A., Merad, N., Khadir, A., Bendahou, M., Djabou, N., Costa, J., & Muselli, A. (2018). Chemical composition and biological investigations of *Eryngium triquetrum* essential oil from Algeria. *Chemistry & Biodiversity*, 15(1), e1700343. <https://doi.org/10.1002/cbdv.201700343>
- Mehrabi, M., Khodarahmi, R., & Shahlaei, M. (2017). Critical effects on binding of epidermal growth factor produced by amino acid substitutions. *Journal of Biomolecular Structure & Dynamics*, 35(5), 1085–1101. <https://doi.org/10.1080/07391102.2016.1171799>
- Mejdoub, K., Mami, I. R., Belabbes, R., Dib, M. E. A., Djabou, N., Tabti, B., Benyelles, N. G., Costa, J., & Muselli, A. (2020). Chemical variability of *Atractylis gummifera* essential oils at three developmental stages and investigation of their antioxidant, antifungal and insecticidal activities. *Current Bioactive Compounds*, 16(4), 489–497. <https://doi.org/10.2174/1573407215666190126152112>
- Mesli, M., & Bouchentouf, S. (2019). Virtual screening of natural and synthetic inhibitors of cyclooxygenase COX-2 enzyme using docking-scoring functions. *Journal of Applied Pharmaceutical Science*, 9(01), 020–027.
- Mesli, F., Daoud, I., & Ghalem, S. (2019). Antidiabetic activity of *Nigella Sativa* (BLACK SEED)-by molecular modeling elucidation, molecular dynamic, and conceptual DFT investigation. *Pharmacophore*, 10(5), 57–66.
- Mesli, F., & Ghalem, S. (2017). Comparative studies of chromen derivatives by using numerical methods. *Asian Journal of Chemistry*, 29(7), 1405–1412. <https://doi.org/10.14233/ajchem.2017.20363>
- Naegeli, P., & Weber, G. (1970). The total synthesis of racemic davanone. *Tetrahedron Letters*, 11(12), 959–962. [https://doi.org/10.1016/S0040-4039\(01\)97878-5](https://doi.org/10.1016/S0040-4039(01)97878-5)
- Naz, S., Farooq, U., Khan, S., Sarwar, R., Mabkhot, Y. N., Saeed, M., Alsayari, A., Muhsinah, A. B., & Ul-Haq, Z. (2020). Pharmacophore model-based virtual screening, docking, biological evaluation and molecular dynamics simulations for inhibitors discovery against  $\alpha$ -tryptophan synthase from *Mycobacterium tuberculosis*. *Journal of Biomolecular Structure and Dynamics*. <https://doi.org/10.1080/07391102.2020.1715259>
- Neidle, S. (2001). DNA minor-groove recognition by small molecules. *Natural Product Reports*, 18(3), 291–309. <https://doi.org/10.1039/a705982e>
- Parikesit, A. A., Nugroho, A. S., Hapsari, A., & Tambunan, U. S. F. (2015). The computation of cyclic peptide with prolin-prolin bond as fusion inhibitor of DENV envelope protein through molecular docking and molecular dynamics simulation. *arXiv preprint arXiv:1511.01388*.
- Petersson, A., Bennett, A., Tensfeldt, T. G., Al-Laham, M. A., Shirley, W. A., & Mantzaris, J. (1988). A complete basis set model chemistry. I. The total energies of closed-shell atoms and hydrides of the first-row elements. *Journal of Chemical Physics*, 89(4), 2193–2218. <https://doi.org/10.1063/1.455064>
- Polo, S., Tardío, J., Vélez-del-Burgo, A., Molina, M., & Pardo-de-Santayana, M. (2009). Knowledge, use and ecology of golden thistle (*Scolymus hispanicus* L.) in Central Spain. *Journal of Ethnobiology and Ethnomedicine*, 5(1), 42. <https://doi.org/10.1186/1746-4269-5-42>
- Quezel, P., Santa, S., & Schotter, O. (1962). *Nouvelle flore de l'Algérie et des régions désertiques méridionales-v.1-2*. Editions du Centre National de la recherche scientifique.
- Ramezani, M., Behravan, J., & Yazdinezhad, A. (2005). Chemical composition and antimicrobial activity of the volatile oil of *Artemisia khorasanica* from Iran. *Pharmaceutical Biology*, 42(8), 599–602. <https://doi.org/10.1080/13880200490902482>
- Rasouli, H., Norooznejhad, A. H., Rashidi, T., Hoseinkhani, Z., Mahnam, A., Tarlan, M., Moasefi, N., Mostafaei, A., & Mansouri, K. (2018). Comparative in vitro/theoretical studies on the anti-angiogenic activity of date pollen hydro-alcoholic extract: Highlighting the important roles of its hot polyphenols. *BioImpacts: Bi*, 8(4), 281–294. <https://doi.org/10.15171/bi.2018.31>
- Ravi, L., & Krishnan, K. (2016). Cytotoxic potential of N-hexadecanoic acid extracted from *Kigelia pinnata* leaves. *Asian Journal of Cell Biology*, 12(1), 20–27. <https://doi.org/10.3923/ajcb.2017.20.27>
- Rustaiyan, A., Masoudi, S., & Kazemi, M. (2007). Volatile oils constituents from different parts of *Artemisia ciniformis* Krasch. et M. Pop. ex Poljak and *Artemisia incana* (L.) Druce. from Iran. *Journal of Essential Oil Research*, 19(6), 548–551. <https://doi.org/10.1080/10412905.2007.9699328>
- Rustaiyan, A., Tabatabaei-Anaraki, M., Kazemi, M., Masoudi, S., & Makipour, P. (2009). Chemical composition of essential oil of three *Artemisia* species growing wild in Iran: *Artemisia kermanensis* Podl., *A. kopetdaghensis* Krasch., *M. Pop et Lincz. ex Poljak.*, and *A. haussknechtii* Boiss. *Journal of Essential Oil Research*, 21(5), 410–413.
- Saikia, A. K., & Sahoo, R. K. (2011). Chemical composition and antibacterial activity of essential oil of *Lantana camara* L. *Middle-East Journal of Scientific Research*, 8(3), 599–602.
- Saljooghianpour, M., & Javaran, T. A. (2013). Identification of phytochemical components of aloe plantlets by gas chromatography-mass spectrometry. *African Journal of Biotechnology*, 12(49), 6876–6880.
- Servi, H. (2019). Essential oil composition from aerial parts of *Scolymus hispanicus* L. *Aurum Journal of Health Sciences*, 1(2), 87–94.
- Sipma, G., & Van der Wal, B. (2010). The structure of davanone a new sesquiterpene from davana: (*Artemisia pallens*, Wall.). *Recueil Des Travaux Chimiques Des Pays-Bas*, 87(6), 715–720. <https://doi.org/10.1002/recl.19680870613>
- Stewart, J. J. (2007). Optimization of parameters for semiempirical methods V: Modification of NDDO approximations and application to 70 elements. *Journal of Molecular Modeling*, 13(12), 1173–1213. <https://doi.org/10.1007/s00894-007-0233-4>
- Stitou, M., Toufik, H., Bouachrine, M., & Lamchouri, F. (2020). Quantitative structure–activity relationships analysis, homology modeling, docking and molecular dynamics studies of triterpenoid saponins as Kirsten rat sarcoma inhibitors. *Journal of Biomolecular Structure and Dynamics*. <https://doi.org/10.1080/07391102.2019.1707122>
- Sturgeon, J. B., & Laird, B. B. (2000). Symplectic algorithm for constant-pressure molecular dynamics using a Nosé–Poincaré thermostat. *Journal of Computational Physics*, 112(8), 3474–3482.
- Tabet Zatlá, A., Dib, M. E. A., Djabou, N., Tabti, B., Meliani, N., Costa, J., & Muselli, A. (2017). Chemical variability of Essential oil of *Daucus carota* subsp. *sativus* from Algeria. *Journal of Herbs, Spices & Medicinal Plants*, 23(3), 216–230. <https://doi.org/10.1080/10496475.2017.1296053>
- Thomas, A. F., Thommen, W., Willhalm, B., Hagaman, E. W., & Wenkert, E. (1974). Terpenoids derived from linalyl oxide. Part 1. The stereochemistry of the davanones. *Helvetica Chimica Acta*, 57(7), 2055–2061. <https://doi.org/10.1002/hlca.19740570716>
- Tresaugues, L., Roos, A., Arrowsmith, C., Berglund, H., Bountra, C., Collins, R., Hammarstrom, M., Edwards, A. M., Flodin, S., Flores, A., Graslund, S., Johansson, A., Johansson, I., Karlberg, T., Kotenyova, T., Moche, M., Nyman, T., Persson, C., Kragh-Nielsen, T., ... Nordlund, P. (2013). Crystal structure of VEGFR1 in complex with N-(4-Chlorophenyl)-2-((pyridin-4-ylmethyl) amino) benzamide. *The RCSB Protein Data Bank*. <https://doi.org/10.2210/pdb3HNG/pdb>
- Vázquez, F. M. (2000). The genus *Scolymus* tourn ex I (asteraceae): Taxonomy and distribution. *Anales Del Jardín Botánico de Madrid*, 58(1), 83–100. <https://doi.org/10.3989/ajbm.2000.v58.i1.139>

Walker, C. B. (1996). The acquisition of antibiotic resistance in the periodontal microflora. *Periodontology*, 2000, 10(1), 79–88. <https://doi.org/10.1111/j.1600-0757.1996.tb00069.x>

Wan, K. K., Evans-Klock, C. D., Fielder, B. C., & Vosburg, D. A. (2013). Synthesis of cis- and trans-Davanoids: Artemone, Hydroxydavanone, Isodavanone, and Nordavanone. *Synthesis*, 45(11), 1541–1545.